

Cell wide responses to low oxygen exposure in *Desulfovibrio vulgaris* Hildenborough

Aindrita Mukhopadhyay^{1,2}, Alyssa M. Redding^{†1,3}, Marcin P. Joachimiak^{†1,2}, Adam P. Arkin^{1,2,4}, Sharon E. Borglin^{1,5}, Paramvir S. Dehal^{1,2}, Romy Chakraborty^{1,5}, Jil T. Geller^{1,5}, Terry C. Hazen^{1,5}, Qiang He^{1,6} [€], Dominique C. Joyner^{1,5}, Vincent J. J. Martin^{1,2, ‡}, Judy D. Wall^{1,7}, Zamin Koo Yang^{1,6}, Jizhong Zhou^{1,6, 8}, Jay D. Keasling^{1,2,3,4 *}

¹Virtual Institute of Microbial Stress and Survival, ²Physical Biosciences Division, Lawrence Berkeley National Laboratory, Berkeley, USA, ³Department of Chemical Engineering, University of California, Berkeley, USA, ⁴Department of Bioengineering, University of California, Berkeley, USA, ⁵Earth Sciences Division, Lawrence Berkeley National Laboratory, Berkeley, USA, ⁶Environmental Sciences Division, Oak Ridge National Laboratory, Oak Ridge, TN, USA, ⁷Biochemistry and the Molecular Microbiology & Immunology Departments, University of Missouri, Columbia, USA, ⁸Institute for Environmental Genomics and Department of Botany and Microbiology, Oklahoma University, Norman, OK, USA, .

*Corresponding author:

Jay D. Keasling, Berkeley Center for Synthetic Biology, 717 Potter Street, Berkeley, CA, 94720 USA, Email: keasling@berkeley.edu, Phone: 510-495-2620, Fax: 510-495-2630

[†] These authors contributed equally to this study.

- 1 ‡Present Address: Biology Department, Centre for Structural and Functional Genomics,
- 2 Concordia University, 7141 Sherbrooke West, Montreal, Quebec, Canada, H4B 1R6
- 3 € Present Address: Department of Civil and Environmental Engineering, Temple University,
- 4 Philadelphia, PA 19122

1 ABSTRACT

2 The responses of the anaerobic, sulfate-reducing *Desulfovibrio vulgaris* Hildenborough to
3 low oxygen exposure (0.1% O₂) were monitored via transcriptomics and proteomics. Exposure
4 to 0.1% O₂ caused a decrease in growth rate without affecting viability. A concerted up-
5 regulation in the predicted peroxide stress response regulon (PerR) genes was observed in
6 response to the 0.1% O₂ exposure. Several of these candidates also showed increases in protein
7 abundance. Among the remaining small number of transcript changes was the upregulation of the
8 predicted transmembrane tetraheme cytochrome *c*₃ complex. Other known oxidative stress
9 response candidates remained unchanged during this low O₂ exposure. To fully understand the
10 results of the 0.1% O₂ exposure, transcriptomics and proteomics data were collected for exposure
11 to air using a similar experimental protocol. In contrast to the 0.1% O₂ exposure, air exposure
12 was detrimental to both the growth rate and viability and caused dramatic changes at both the
13 transcriptome and proteome levels. Interestingly, the transcripts of the predicted PerR regulon
14 genes were down regulated during air exposure. Our results highlight the differences in the cell
15 wide response to low and high O₂ levels of in *D. vulgaris* and suggest that while exposure to air
16 is highly detrimental to *D. vulgaris*, this bacterium can successfully cope with periodic exposure
17 to low O₂ levels in its environment.

18
19 **Key words:** PerR regulon, oxygen, air, stress, iTRAQ, microarray, integrated functional
20 genomics, sulfate reducing bacteria.

INTRODUCTION

Sulfate reducing bacteria (SRB) like *Desulfovibrio spp.* are truly cosmopolitan organisms that flourish in deep subsurface sediments, rice paddies, lake and ocean sediments, insect and animal guts, sewers and oil pipelines (8, 27, 40, 41, 51). Though considered obligate anaerobes for many years after their discovery, *Desulfovibrio spp.* are found in many environments that are regularly or periodically exposed to oxygen (8, 20, 35). A number of *Desulfovibrio spp.* have been documented to reduce millimolar levels of O₂ (12), and in an O₂ gradient, *Desulfovibrio vulgaris* Hildenborough localizes to very low O₂ concentrations rather than the anoxic region (30). However, *D. vulgaris* does not couple growth to O₂ respiration (8, 12), and even small amounts of O₂ affect growth adversely (57). Although *D. vulgaris* has been shown to survive long periods of air exposure (8, 9), it grows optimally in an anaerobic environment (46).

Several studies have focused on discovering the *D. vulgaris* genes involved in its oxidative stress response (7, 36), and a basic model for O₂ stress response in *D. vulgaris* has been proposed and reviewed (7, 37). *D. vulgaris* has two major mechanisms for superoxide removal, namely the superoxide reductase (Sor) and the superoxide dismutase (Sod). The Sor, also called desulfoferrodoxin or rubredoxin oxidoreductase (*rbo*), occurs as part of an operon that also encodes a rubredoxin (*rub*) and the rubredoxin oxygen oxidoreductase (*roo*). The Sor reportedly works in conjunction with peroxidases (e.g., AhpC, rubrerythrins (18, 37)) and electron transfer proteins such as rubredoxins (7) to convert superoxides to water. With regard to reactive oxygen species (ROS) removal, the Sor mechanism is considered to be the preferred pathway as it does not regenerate any intracellular O₂ (14, 26, 28, 42). The *D. vulgaris* genome encodes multiple genes, such as rubrerythrins, rubredoxins, and a nigerytherin, that are anticipated to be involved in peroxide reduction (Figure 1). The sequence analysis of the *D. vulgaris* genome (23) enabled

1 prediction of regulons, among which a putative PerR regulon was defined (49). The inferred
2 PerR regulon contains the *perR* regulator and a subset of the peroxide reduction genes mentioned
3 above (*ahpC*, *rbr*, *rbr2*, *rhl* and a conserved hypothetical protein, Figure 1). The *D. vulgaris*
4 genome also encodes a Fe-Sod that has been shown to provide a protective mechanism in the
5 periplasmic space where O₂-sensitive enzymes, such as the Fe-hydrogenase (HydA/B), function
6 (17, 54). The *D. vulgaris* Sod may also work in conjunction with a catalase, an efficient enzyme
7 that catalyzes the turnover of H₂O₂ to water and oxygen (42). Interestingly, the *D. vulgaris*
8 catalase is encoded on a 202-kb plasmid, which has been documented to be lost during growth in
9 ammonium-rich medium (18).

10 Despite these protective mechanisms, ROS, such as superoxides and peroxides, are still
11 produced during O₂ reduction and trigger a variety of cellular damages in both aerobic and
12 anaerobic organisms (37, 45, 53). While it is the ROS that cause the majority of O₂ related
13 damage, O₂ itself also irreversibly deactivates critical periplasmic proteins such as reduced Fe-
14 hydrogenases (54). Oxidative stress due to O₂ exposure is known to have multiple effects on
15 cellular physiology, and O₂ exposure at both high and low levels can be expected to elicit
16 cellular responses, especially for anaerobic organisms. Our current knowledge of the oxidative
17 stress response mechanisms in *D. vulgaris* is derived mainly from studies conducted using air or
18 100% O₂ exposure (13, 16-18, 59). A survey of these studies also revealed that differences in
19 experimental protocols led to important differences in cellular responses. For example, a study
20 of oxygen responsive genes in *D. vulgaris* (18) reported a loss of viability in response to air
21 exposure, yet a similar microarray study of air exposure (59) observed no such loss. Further, the
22 modulation of the multiple protective mechanisms in response to low O₂ exposure was not
23 explored. The specificity of many of these mechanisms in O₂ exposure also remains undefined,

1 as many of the candidate proteins are intimately linked with the redox status of the cell and may
2 have redundant functions.

3 We hypothesized that a cell-wide study of *D. vulgaris* in a low oxygen environment
4 might uncover new information about these mechanisms. Consistent with this, a recent study
5 showed a *roo* mutant to be sensitive to 0.2% O₂ exposure (57). Cell-wide data from an air stress
6 response may provide the perspective required to determine the specificity of responses in the
7 low O₂ exposure. In order to minimize variability from experimental setup and to place our data
8 in context of previous studies, we conducted controlled experiments to measure *D. vulgaris*
9 responses to both low oxygen levels and air.

10 **MATERIALS and METHODS**

11 *Bacterial growth and maintenance.* Bacterial strains were grown and maintained as
12 described previously (39). In brief, *Desulfovibrio vulgaris* Hildenborough (ATCC 29579) was
13 grown in a defined lactate (60 mM)/sulfate (50 mM) medium, LS4D (39). To minimize sub-
14 culturing during experimentation, *D. vulgaris* stocks stored at -80°C were used as a 10% (% is
15 v/v unless otherwise indicated) inoculum into 100-200 mL of fresh LS4D medium and the cells
16 were grown to mid-log phase (optical density at a wavelength of 600 nm (OD₆₀₀) of 0.3 – 0.4).
17 For every transcriptome and proteome experiment, fresh starter cultures at mid-log phase were
18 used as 10% inoculum into 1-3 L biomass production cultures and grown at 30°C, as noted
19 previously (39).

20 *Cell counts and growth assays during air and 0.1% O₂ exposure.* One L of *D. vulgaris*
21 culture in LS4D medium at mid-log phase (OD₆₀₀ = 0.35) was sparged with either humidified,
22 sterile N₂, 0.1% O₂ in N₂, or air (21% O₂). The sparge bottles were constructed from 2-L media

bottles with three-valve standard HPLC delivery caps (ULTRA-WARE, Kimble/Kontes). One valve was used to allow gas to enter, another for sampling, and the third for gas venting. Gas was sparged through porous Teflon tubing (International Polymer Engineering, Tempe AZ) filled with glass micro beads to keep the tubing submerged in the culture. Samples were taken at 0, 60, 120, and 240 min following exposure. For measuring growth, cells were counted using the acridine orange direct count (AODC) method (31). For measuring viability, colony forming units (CFU) were tested, for which aliquots were taken at the above time points and diluted serially in anaerobic LS4D medium to obtain 10^2 and 10^4 dilutions. A 200 μ L sample of each dilution was suspended in molten LS4D containing 0.8% (w/v) agar before being spread on LS4D plates containing 1.5% (w/v) agar and grown anaerobically; colonies were counted after seven days.

Biomass production for integrated 'omics' experiments. Biomass for microarray analysis and proteomics experiments was generated as described previously (39). All production cultures were grown in triplicate. At an OD₆₀₀ of 0.3 (initial time point, T₀), sample triplicates were collected (300 mL each for microarrays and 50 mL each for proteomics). Once T₀ sampling was completed, the stress was applied by sparging humidified, sterile air, 0.1% O₂ in N₂, air or N₂ (control) at approximately 200 mL/min through the 2 L cultures. Prior to T₀, the doubling time for *D. vulgaris* was measured to be approximately 5 hours. Samples were collected at 30, 60, 120, and 240 min after sparging was initiated. Processing and chilling times were minimized by pumping samples through a metal coil immersed in an ice bath as described previously (39). The chilled samples were harvested via centrifugation, flash frozen in liquid nitrogen, and stored at -80°C until analysis. Consistent with previous studies (18), pH measurements during sparging indicated that all treatments (N₂, 0.1% O₂, or air) resulted in a small pH (< 0.8) increase that may have been caused by H₂S and CO₂ loss during sparging. After four hours, the pH of each culture

1 was between 7.8 and 8.0. Using previously reported specific oxygen reducing potential of wild
2 type *D. vulgaris* (57), it could be estimated that the maximum oxygen reducing potential of the
3 culture is approximately 5.4 $\mu\text{mol O}_2$ / min. At a sparging rate of 200 mL /min, 7.8 $\mu\text{mol O}_2$ /
4 min is estimated to be added to the culture (Supplementary data, Calculation S1,
5 <http://vimss.lbl.gov/Oxygen/>). Measurements with Foxy Fospo-R oxygen sensor (Ocean Optics,
6 Florida, USA) indicated that a continuous sparge with 0.1% O_2 increased the levels of dissolved
7 O_2 in the blank media. The higher levels of O_2 (relative to the pure N_2 sparge) were detectable in
8 a live *D. vulgaris* culture while being sparged, and ensured that there was a constant exposure to
9 O_2 during the 0.1% O_2 treatment (Supplementary data, Figure S2, <http://vimss.lbl.gov/Oxygen/>).

10
11 *Microarray transcriptomic experiments and data analysis.* DNA microarrays using 70-
12 mer oligonucleotide probes covering 3,482 of the 3,531 annotated protein-coding sequences of
13 the *D. vulgaris* genome were constructed as previously described (33). Briefly, all
14 oligonucleotides were commercially synthesized without modification by MWG Biotech Inc.
15 (High Point, NC), prepared in 50% vol/vol DMSO (Sigma-Aldrich, St Louis, MO) and spotted
16 onto UltraGAPS glass slides (Corning Life Sciences, Corning, NY) using a BioRobotics
17 Microgrid II microarrayer (Genomic Solutions, Ann Arbor, MI). Each oligonucleotide probe
18 had two replicates on a single slide. Probes were fixed onto the slides by UV cross-linking (600
19 mJ) according to manufacturer's protocol. Total RNA extraction, purification, and labeling were
20 performed independently on each cell sample using previously described protocols (5). Each
21 replicate sample consisted of cells from 300 mL cultures. Labeling of cDNA targets from
22 purified total RNA was carried out using the reverse transcriptase reaction with random hexamer
23 priming and the fluorophore Cy5-dUTP (Amersham Biosciences, Piscataway, NJ). Genomic

1 DNA was extracted from *D. vulgaris* cultures at stationary phase and labeled with the
2 fluorophore Cy3-dUTP (Amersham Biosciences, Piscataway, NJ). To hybridize a single glass
3 slide, the Cy5-dUTP-labeled cDNA probes obtained from stressed or unstressed cultures were
4 mixed in equal amounts with the Cy3-dUTP-labeled genomic DNA. After washing and drying,
5 the microarray slides were scanned using the ScanArray Express microarray analysis system
6 (Perkin Elmer). The fluorescent intensity of both the Cy5 and Cy3 fluorophores was analyzed
7 with ImaGene software version 6.0 (Biodiscovery, Marina Del Rey, CA).

8 Microarray data analyses were performed using gene models from NCBI. All mRNA
9 changes were assessed with total genomic DNA as control. Log₂ ratios and z-scores were
10 computed as previously described (39). A mean log₂-ratio cutoff of $\geq |2|$ across time points and
11 an accompanying z-score $\geq |2|$ were used to identify genes whose expression changed most
12 significantly. Searches of the microarray data with the mean gene expression profile of genes in
13 the predicted PerR regulon were performed using the Pearson correlation coefficient as the
14 scoring function and the Euclidean distance to sort the final search results. The 0.71 correlation of
15 the rubredoxin-like protein DVU3093, the lowest scoring gene from the predicted PerR regulon,
16 was used as an empirical significance cutoff for the profile search results. (For additional notes
17 and analysis information see supplementary Figure S5). All heat-maps of gene expression data
18 were rendered as vector graphics and output in Encapsulated PostScript (EPS) format using
19 JColorGrid (29). The rendering configuration specified a constant maximum and minimum data
20 range (log₂ ratio range of (-6.25, 6.25)), a log₂ ratio increment of 0.5, and with the log₂ ratio
21 color scale centered at log₂ ratio = 0.

22 The specificity of transcription changes in the predicted PerR regulon genes was assessed
23 using the mean expression of genes in the regulon computed across different experimental

conditions corresponding to six previously published VIMSS studies (e.g., heat shock (5), salt stress (39), nitrite (22), and stationary phase (6)). The mean expression of genes in the PerR regulon was computed for each time point in each experiment, as well as the global mean and standard deviation across all time points and experiments. To assess the confidence of the observed gene expression changes, z-scores were computed for the mean PerR gene expression at each time point in the 0.1% O₂ and air stress experiments. Assuming a normal distribution, the 95% confidence interval corresponds to a z-score of 2, and at most 5% of the data are expected to have more significant changes. In the microaerobic experiment the z-scores were 0.4, 1.2, and 1.7 for time points 60, 120, and 240 min, respectively. In the air stress experiment, the z-scores were -0.4 -0.8, -1.3, -1.6, and -2.5, for time points 0, 10, 30, 120, and 240 min, respectively. Note that this is the only calculation of z-score across multiple experiments; all other z-scores reported in this study have been computed across the 0.1% O₂ and air exposure experiments only. Microarray data for this study is available through the URL: <http://www.microbesonline.org/cgi-bin/microarray/viewExp.cgi?locusId=&expId=28+74>. Raw microarray data can also be accessed through the following URLs for 0.1% O₂ exposure and air stress respectively; http://www.microbesonline.org/microarray/rawdata/exp28_E35 http://www.microbesonline.org/microarray/rawdata/exp74_E12

Proteomics and proteomics data analyses. Sample preparation, chromatography, and mass spectrometry for iTRAQ proteomics were performed as described previously (47) with modifications to the lysis buffers used. Frozen cell pellets from triplicate 50 mL cultures were thawed and pooled prior to cell lysis. For the 0.1% O₂-exposed biomass, cells were lysed via sonication in 500 mM triethylammonium bicarbonate (TEAB), pH 8.5 (Sigma-Aldrich), and the clarified lysate was used as total cellular protein. Sample denaturation, reduction, blocking,

1 digestion, and labeling with isobaric reagents were performed according to the manufacturer's
2 directions (Applied Biosystems, Framingham, MA). The four-plex iTRAQ labels were used as
3 follows: tag₁₁₄, T₀ control; tag₁₁₅, 240-minute control; tag₁₁₆, 240-minute 0.1% O₂ sparged; and
4 tag₁₁₇, 240-minute 0.1% O₂ sparged (replicate). Tag₁₁₆ and tag₁₁₇ provided technical replicates to
5 allow assessment of internal error. For the air-exposed biomass, cell pellets were lysed via
6 sonication in lysis buffer (4 M urea, 500 mM TEAB, pH 8.5), and the clarified lysate was diluted
7 with water to 1 M urea before being used. The same labeling procedure was used, and labels
8 were used as follows: tag₁₁₄, 120-minute N₂ sparged control; tag₁₁₅, 240-minute N₂ sparged
9 control; tag₁₁₆, 120-minute air sparged; and tag₁₁₇, 240-minute air sparged. Strong cation
10 exchange (SCX) was used to separate both 0.1% O₂- and air-exposed, iTRAQ-labeled samples
11 into 21-23 salt fractions. Fractions were desalted, dried, and separated on a C₁₈ reverse phase
12 nano-LC-MS column using a Dionex LC system coupled with an ESI-QTOF mass analyzer
13 (QSTAR® Hybrid Quadrupole TOF, Applied Biosystems, Framingham, MA) as previously
14 described (47).

15 Collected mass spectra were analyzed using Analyst 1.1 with ProQuant 1.1, ProGroup
16 1.0.6 (Applied Biosystems, Framingham, MA), and MASCOT version 2.1 (Matrix Science, Inc,
17 Boston, USA). A FASTA file containing all the putative ORF sequences of *D. vulgaris*, obtained
18 from microbesonline.org (1) was used to form the theoretical search database along with the
19 common impurities trypsin, keratin, cytochrome *c*, and bovine serum albumin. The same search
20 parameters were used in both programs as described previously (47). Only proteins identified by
21 at least two unique peptides at greater than 95% confidence by both ProQuant and MASCOT
22 were considered for further analysis.

All protein ratios were obtained from the ProQuant database using ProGroup. Tag ratios for each protein were computed as the weighted average from all peptides that were uniquely assigned to that protein. Technical replicates (tag₁₁₆ and tag₁₁₇ used to label 0.1% O₂ exposed biomass) were used to assess variability in quantification of Log₂ ratios. To define a cut-off for internal error, the deviation between the absolute value of log₂(116/115) and log₂(117/115) for a given protein was used. The internal error cut-off was set at the value of deviation at which 95% of all proteins showed deviation \leq that value. The internal error cut-off was found to be |0.13|. To compute the level of significant change, z-score was computed for all log₂ values. Protein log₂ values with z-scores \geq |2| were considered to be significantly changed. COG categories as defined by (52) were used to plot fraction of each COG category identified (Figure 8). Complete proteomics data can be obtained at <http://vimss.lbl.gov/Oxygen/>

RESULTS

Effect of different growth conditions on biomass and viability. For genome-wide assessment of cellular response, growth assays were conducted to determine the level of O₂ that affected the growth rate but was not lethal. Extended exposure to 0.05% O₂ had no overall effect on *D. vulgaris* growth (Figure 2A). Consistent with this, there were no significant changes in transcript levels under these conditions (Supplementary data, <http://vimss.lbl.gov/Oxygen/>). Sparging with 0.1% O₂ reduced both the growth rate and maximal growth (Figure 2A). However the cells resumed normal growth after a lag of about three growth cycles (15 hours), and colony forming units (CFU) were similar to control (Supplementary Figure S1, 3). Therefore, 0.1% O₂ was selected as the condition for the low O₂ exposure experiments in this study. Though the affect of 0.1% O₂ exposure on growth was most evident at later time points, to measure cellular

1 response at the transcript and protein level, biomass was collected at time points up until 240
2 minutes post exposure Figure 2B).

3 When exposed to air (21% O₂) for a similar length of time, the effect on both growth rate
4 and viability was drastic. Direct cell counts showed that the air sparged samples contained only
5 40% of the number of cells present in the control (N₂ sparge) after 240 minutes of sparging.
6 Further, a measurement of the CFU indicated that only a fraction of cells formed colonies when
7 plated (~ 10%) compared the control culture at T₀ (Supplementary Figure S3). This result is
8 consistent with most previous studies where a similar reduction in viability has been documented
9 (18); there was only one exception where colony forming units remained unaffected (59).

10 *Genome wide transcriptional response.* The transcript profiles of cultures exposed to
11 0.1% O₂ were analyzed. Applying a log₂ ratio cutoff of $\geq |2|$ in at least one time point (and $z \geq$
12 $|2|$), for genes whose expression changed significantly, revealed only 12 significantly up-
13 regulated genes. These results suggest that 0.1% O₂ exposure produced a mild perturbation in *D.*
14 *vulgaris*. The up-regulated genes included five out of the six predicted members of the predicted
15 PerR regulon (Figure 3). Few other genes with annotated functions showed a significant change;
16 however, *tmcB* (DVU0264) and *divK* (DVU0259), were upregulated, both of which belong to an
17 operon containing an iron sulfur cluster transmembrane ferredoxin complex. Using the same
18 criteria, no transcript showed significant down regulation.

19 It is noteworthy that following an exposure to 0.1% O₂, the *perR* transcript increased with
20 time, as did the transcripts of all other predicted PerR regulon genes (Figure 3). In addition to
21 the predicted PerR regulon, the *D. vulgaris* genome encodes many genes thought to protect
22 against oxidative damage that are widely present across many classes of bacteria, including
23 superoxide dismutase (*sodB*), catalase (*kat*), and several thioredoxins (Figure 4). Based on

conservation across sulfate-reducing bacteria, several oxidative stress response genes are considered to be signature genes in SRB (5) and include predicted oxygen response candidates such as the Sor operon and several ferritins (Figure 5). Of genes encoding functions inferred to protect against oxidative damage, neither the genes widely distributed nor the signature genes showed a significant transcript change in response to 0.1% O₂ exposure. Microarray data also indicated that genes predicted to be involved in central metabolic pathways, such as the sulfate reduction pathway, ATP synthesis, and several periplasmic or cytoplasmic hydrogenases, were unaffected during 0.1% O₂ exposure (Figure 4 and 5).

In contrast, air exposure generated a large number of differentially expressed genes: 393 candidates showed a significant up-regulation whereas 454 genes were found to be down-regulated (for complete data see microarray data link provided in the methods section). Among these, genes in the predicted PerR regulon were downregulated, as were signature SRB genes and other genes considered to provide protection from oxidative stress (Figure 3, 4, 5). Further, in contrast to the response in the 0.1% O₂ exposure, significant down regulation for many genes in central pathways were recorded in air exposure (Figure 4, 5), highlighting the striking difference in *D. vulgaris* response to the two conditions. Upregulated transcripts in the air-stressed biomass included *clp* proteases, chaperone proteins, and phage shock proteins (Figure 8), suggestive of a drastic stress response. None of these genes showed any change during exposure to 0.1% O₂.

Proteomic response. An iTRAQ proteomics strategy was used to identify differences in protein content for the same samples used for microarray analysis. A total of 251 proteins were identified by two independent MS analysis software packages (see Materials and Methods and (47)). As in the microarray data, proteins were considered to be significantly changing if their

absolute z-scores exceeded two. Responses at the protein level may lag those at the transcript level and this may account for the milder proteomic changes compared to microarray results. The highest change noted was over two fold (\log_2 ratio = 1.37). For z-scores $\geq |2|$ there were only four proteins with increased levels and two proteins with decreased levels. Three of the six predicted PerR regulon members were identified in the proteomics data, and all were present at higher levels in the 0.1% O₂ exposed biomass (Figure 6, Table 1). Proteins for other oxygen response mechanisms, such as Sod (DVU2410), RoO (DVU3185) and members of the Sor operon were also identified but no significant changes were observed. The only other protein that showed accumulation in 0.1% O₂ exposure was a putative zinc-resistance associated protein, ZraP (DVU3384), though the mRNA levels did not reflect this change. Only two proteins, Rho (DVU1571), a predicted transcription termination factor, and IlvE (DVU3197), a predicted branched-chain amino acid aminotransferase, showed decreased levels. While many members of central metabolism (e.g., ATP synthesis, sulfate reduction, and pyruvate to acetate conversion) were identified, none of these proteins showed any significant change in response to the 0.1% O₂ exposure, consistent with microarray data.

Proteomics analysis of air-stressed biomass was conducted at both 120 min and 240 min. As can be seen in Figure 6C, the response at 120 min showed a similar trend to that at 240 min. A total of 438 proteins were identified in this analysis. Thirty-three proteins exhibited significant change after 120 min of air sparging, while sixteen changed following 240 min (Table 1). In contrast to the 0.1% O₂ exposure, in air stress, Sod (DVU2410) showed the largest increase and this increase was confirmed by immunoblotting (Supplementary Figure S4, <http://vimss.lbl.gov/Oxygen/>). The proteomics data from the air-stressed biomass also identified proteins in most central pathways (Table 1); however, no concerted significant changes could be

1 seen across any pathways. Notably, neither the ORF annotated as ZraP nor the predicted PerR
2 regulon showed any significant change at 240mins during air exposure.

3 *The PerR regulon expression profile.* The genes of the predicted PerR regulon showed a
4 distinct expression pattern in both the 0.1% O₂ exposure and aerobic stress across several time
5 points (Figure 9). The mean expression profile for the predicted PerR regulon genes was used to
6 search the remainder of the microarray data for other transcripts showing similar changes. Many
7 transcripts correlated with the mean expression profile of the predicted PerR regulon genes
8 across the two conditions and sets of time points. Among the genes of the predicted PerR
9 regulon, the most correlated gene to that of the mean PerR profile was rubrerythrin (DVU3094,
10 correlation 0.98) and the least correlated was a rubredoxin-like protein (DVU3093, 0.71). Using
11 0.71 as an empirical score significance cutoff, the PerR mean expression profile search identified
12 58 candidates. As evidence of the specificity of the information contained in the mean PerR
13 expression profile, we analyzed the score distribution of the PerR regulon members in the search
14 results. The top five out of six candidates from the search were five out of six members of the
15 PerR regulon: a rubrerythrin (DVU3094) (Pearson rank/final rank 1/2, correlation 0.98), *ahpC*
16 (2/1, 0.95), PerR (3/6, 0.94), a hypothetical protein DVU0772 (5/1, 0.89), and a putative
17 rubrerythrin DVU2318 (6/58, 0.89) (Figure 9 and supplementary data, Figure S5 and Table S1).
18 Six out of eight transcripts in the predicted *tmc* operon, encoding the tetraheme cytochrome *c*₃
19 complex, also showed high correlation with the PerR profile: DVU0260 (0.83), DVU0265
20 (0.83), DVU0267 (0.82), DVU0264 (0.80), DVU0266 (0.77), and DVU0263 (0.75). The *cydA/B*
21 genes that encode the putative cytochrome bd oxidase were also correlated with the mean PerR
22 regulon gene expression profile, at 0.74 and 0.69 for *cydA* and *cydB*, respectively (however,
23 *cydB* was correlated below the level of the empirical correlation cutoff). The remaining genes in

the top matches of the profile search were ten conserved hypothetical proteins and thirty seven hypothetical proteins (Table S1, <http://vimss.lbl.gov/Oxygen/>).

DISCUSSION

While continuous bubbling of the *D. vulgaris* culture with 0.1% O₂ ensured cell exposure to a proportional amount of O₂, this level of O₂ exposure produced only a mild perturbation. This is reflected in the small number of genes that changed expression and the fact that no changes were observed in central metabolic genes. This may be an indication that under normal growth conditions, *D. vulgaris* already contains adequate levels of most of the enzymes required to respond to low levels of O₂ exposure. A concerted upregulation of the entire predicted PerR regulon was observed during 0.1% O₂ exposure, with *ahpC* being one of the most upregulated candidates at both the transcript and protein levels. Along with the *tmc* transmembrane cytochrome *c*₃ operon, these were the only cellular responses to 0.1% O₂ exposure. PerR regulons have been described in many bacteria (3, 21, 24, 25, 48, 58), and genes regulated by PerR are often involved in defense against ROS accumulation. In *D. vulgaris*, predicted members of the PerR regulon, such as a rubrerythrin (DVU0265), have been identified as important enzymes in exposure to both O₂ as well as other oxidative stresses (18).

The air stress had a much more drastic effect on a cell-wide level. The responses at the mRNA level were reproducible across biological replicates (Figure 10 B). Further, the changes in transcript levels between air stressed biomass at 120 and 240 min were self consistent, having a Pearson correlation of 0.77. The proteomics measurements for the biomass were similarly self consistent, having a Pearson correlation of 0.73 (Figure 6B). The microarray data indicated an overall down-regulation in central metabolic pathways such as sulfate reduction, ATP synthesis,

1 electron transfer, lactate uptake, and conversion of lactate to acetate, none of which were
2 observed in the 0.1% O₂ exposure. The down regulation of genes such as lactate permease and
3 lactate dehydrogenase during air exposure may be representative of cellular stress or a defensive
4 response to prevent use of the electron donor and consequently prevent reduction of oxygen.
5 Most importantly, upon air exposure the transcript levels for the predicted PerR regulon genes
6 decreased overall, where transcripts for *perR* and genes encoding rubrerythrin and the putative
7 rubrerythrin decreased consistently with time and showed 4-fold to 24-fold down regulation.
8 These results highlight a sharp contrast in the response of *D. vulgaris* to 0.1% O₂ compared to air
9 exposure.

10 Using the mean expression profile for the predicted PerR regulon genes across the two
11 exposures, the microarray data were searched for other transcripts with similar expression
12 profiles. The resulting list contained several members of the eight-gene operon encoding the
13 transmembrane tetraheme cytochrome *c*₃ complex (DVU0258:DVU0266) and also the *cydAB*
14 operon (DVU3270-DVU3271), encoding the cytochrome d ubiquinol oxidase proteins. The
15 cytochrome bd oxidase system is typically involved in oxidative phosphorylation, and increases
16 in the transcription of the corresponding genes during oxidative stress have been reported for
17 other anaerobic bacteria, such as *D. gigas* (38), *Moorella thermoacetica* (11), and *Bacteroides*
18 *fragilis* (2). These enzymes also appear to have a protective role in aerobic bacteria such as
19 *Escherichia coli* and *Salmonella* during oxidative stress (15, 34). The existence of cytochrome
20 bd oxidases in *D. vulgaris* has been a matter of historical discussion since pure cultures of *D.*
21 *vulgaris* are unable to grow in oxygen (8). Here, the significant increase observed in transcripts
22 for the electron transfer systems such as the *tmc* cytochrome *c*₃ complex and for the oxidative

1 phosphorylation enzymes like cytochrome bd oxidase may indicate that additional copies of
2 these enzymes serve a protective role during the 0.1% O₂ exposure.

3 Several redox active proteins such as a thiol peroxidase, bacterioferritin, flavodoxin and
4 ferredoxins also correlated with the mean PerR regulon gene expression profile. Since these
5 candidates also increased during 0.1% O₂ exposure, they may also be required for O₂ defense in
6 *D. vulgaris*. Other oxidative response genes, including the rubredoxin (DVU3184), present in the
7 Sor operon, and the Sor itself, were also identified by the gene expression profile search, but no
8 significant up-regulation of these candidates was observed. Of these fifty-eight candidates, more
9 than one third (twenty one), have no predicted functions. Among genes for which a functional
10 annotation exists, several chemotaxis and signal transduction genes were identified. These genes
11 are ideal candidates for further studies to confirm any specific role in oxidative stress response.

12 It has been recently demonstrated that a *roo* deletion strain of *D. vulgaris* was more
13 sensitive to microaerobic stress than the wild type (57); however, we observed no change in
14 expression of this gene at either the transcript or protein level in the 0.1% O₂ exposure
15 experiments. Deletion of the genes encoding Sor and Sod has been shown to create strains with
16 greater O₂ sensitivity (18). While neither of these genes showed a significant transcriptional
17 change during 0.1% O₂ exposure, candidates that confer fitness and ensure survival may already
18 be present and not necessarily show changes in transcript or protein levels. Compared to the
19 0.1% O₂ exposure, air appears to have a severely detrimental effect on cellular growth. It should
20 be noted however that increase in the Sod protein levels, and the few additional upregulated
21 transcripts in oxidative stress response genes (such as putative peptide methionine sulfoxide
22 reductases, *msrA* and *msrB* (DVU0576 and DVU1984)), in the air stressed biomass may be
23 physiologically relevant for the small population of cells that remain viable in the air exposure.

Genes in the predicted PerR regulon have exhibited perturbations in other *D. vulgaris* functional genomics studies (e.g., heat shock (5), salt stress (39), nitrite stress (22), and stationary phase (6)). The increase in all members of this predicted regulon was also seen in heat shock (5), but the time dependent increase shown by these genes appears to be unique to the 0.1% O₂ exposure. Additionally, while a large number of upregulated genes were documented in the heat shock study, the upregulation during 0.1% O₂ exposure of the predicted PerR regulon genes constitutes a much more specific and limited transcriptional response. Taken together, it appears that PerR derepression is the primary *D. vulgaris* response to low O₂ exposure. Interestingly, the air stress transcriptomic data correlated better with that of heat shock than with the data from 0.1% O₂ exposure (Figure 10), and the predicted PerR regulated genes were significantly down regulated in air stress, further supporting the specificity of PerR derepression during low O₂ exposure. The common changes between air stress and heat shock have been also noted in a previous study (59).

Another candidate that was universally upregulated across multiple stress conditions monitored in *D. vulgaris* was a protein annotated as zinc resistance-associated protein ZraP (DVU3384). Though it was highly upregulated in both conditions studied here, DVU3384 may be a general stress response candidate. Additionally, though zinc uptake regulons have been shown to increase in O₂ exposure in *Lactobacilli* (50) and oxidative stress in *Bacillus* (19), DVU3384 may not be a zinc binding protein. In proteins with confirmed zinc binding motifs such as the *E. coli* YjaI, known to preferentially bind Zn and Ni (43), Zn binding is conferred by a two-part motif: an N-terminally located sequence, HRWHGRC, and a C-terminally located sequence, HGGHGMW. Due to the evolutionary distances between this gamma proteobacterium versus the delta sulfate reducer and the low sequence similarity to experimentally validated

1 proteins, more experimental proof is required to confirm the metal ion binding specificity of the
2 *D. vulgaris* ZraP (DVU3384). However, the *D. vulgaris* ZraP sequence contains a cysteine
3 residue in the C-terminal region as well as multiple histidine residues in the N-terminal region,
4 both contained in glycine-rich and presumably flexible regions of the protein. Together these
5 data suggest that the *D. vulgaris* ZraP contains a likely metal binding site and is an interesting
6 candidate for follow up experiments.

7 Many bacteria traditionally categorized as anaerobic organisms, including *Helicobacter*
8 *pylori* (56) and *Bacteroides fragilis* (2), contain numerous mechanisms to counter O₂ stress.
9 Other anaerobes, such as *Clostridium spp*, *Moorella thermoacetica*, and *Spirillum winogradskii*
10 (4, 10, 11, 32, 44), have also been found to tolerate transient exposure to oxic environments.
11 While some among these are microaerophilic, *D. vulgaris*, like *H. pylori* and *Clostridium spp.*,
12 cannot utilize O₂ for growth and is anaerobic by definition. However, our data indicate that this
13 bacterium can survive 0.1% O₂ exposure both in terms of growth as well as cellular response and
14 appears to be entirely suited for ecological niches that experience transient exposure to O₂.
15 Results from previous studies have shown that the members of the Sor operon and other
16 oxidative stress response genes are important for the survival of *D. vulgaris* in O₂ exposure (18,
17 55). Our study suggests that additional protection may be provided by the peroxidases in the
18 predicted PerR regulon and membrane bound cytochromes. The very concerted increase and
19 temporal response of the predicted PerR regulon in *D. vulgaris* upon exposure to low
20 concentrations of oxygen is consistent with a physiological response to a condition that may be
21 frequently encountered in the natural environment. Seasonal episodic infiltration of snow melts
22 and rainfall events bring oxygenated waters to previously established anoxic and reducing
23 environments. Given the ability of *D. vulgaris* to cope with low O₂ levels for short periods, these

1 weather related effects are unlikely to be catastrophic. Further, despite the graver consequences
2 of exposure to higher levels of O₂, even the limited viability ensures propagation of the
3 bacterium through this exceedingly harsh stress. This further suggests why *D. vulgaris* and other
4 SRBs are so resilient in a variety of habitats, including those where exposure to oxygen may
5 occur periodically.

7 **ACKNOWLEDGEMENTS**

8 We are grateful to Morgan Price, Eric Alm and Katherine Huang for helpful discussions.
9 We thank Rick Huang, Richard Phan, and Mary Singer for technical help with biomass
10 production, Barbara Giles for sharing experimental observations, and Keith Keller and Janet
11 Jacobsen for help with the supplementary data link. This work was part Environmental Stress
12 Pathway Project (ESPP) of the Virtual Institute for Microbial Stress and Survival
13 (<http://vimss.lbl.gov>) supported by the U. S. Department of Energy, Office of Science, Office of
14 Biological and Environmental Research, Genomics: GTL Program through contract DE-AC02-
15 05CH11231 with LBNL. Oak Ridge National Laboratory is managed by University of
16 Tennessee-Battelle LLC for the Department of Energy under contract DE-AC05-00OR22725.

REFERENCES

1. Alm, E. J., K. H. Huang, M. N. Price, R. P. Koche, K. Keller, I. L. Dubchak, and A. P. Arkin. 2005. The MicrobesOnline Web site for comparative genomics. *Genome Res* **15**:1015-22.
2. Baughn, A. D., and M. H. Malamy. 2004. The strict anaerobe *Bacteroides fragilis* grows in and benefits from nanomolar concentrations of oxygen. *Nature* **427**:441-4.
3. Brenot, A., K. Y. King, and M. G. Caparon. 2005. The PerR regulon in peroxide resistance and virulence of *Streptococcus pyogenes*. *Mol Microbiol* **55**:221-34.
4. Briolat, V., and G. Reyssset. 2002. Identification of the *Clostridium perfringens* genes involved in the adaptive response to oxidative stress. *J Bacteriol* **184**:2333-43.
5. Chhabra, S. R., Q. He, K. H. Huang, S. P. Gaucher, E. J. Alm, Z. He, M. Z. Hadi, T. C. Hazen, J. D. Wall, J. Zhou, A. P. Arkin, and A. K. Singh. 2006. Global Analysis of Heat Shock Response in *Desulfovibrio vulgaris* Hildenborough. *J Bacteriol* **188**:1817-28.
6. Clark, M. E., Q. He, Z. He, K. H. Huang, E. J. Alm, X. F. Wan, T. C. Hazen, A. P. Arkin, J. D. Wall, J. Z. Zhou, and M. W. Fields. 2006. Temporal transcriptomic analysis as *Desulfovibrio vulgaris* Hildenborough transitions into stationary phase during electron donor depletion. *Appl Environ Microbiol* **72**:5578-88.
7. Coulter, E. D., and D. M. Kurtz, Jr. 2001. A role for rubredoxin in oxidative stress protection in *Desulfovibrio vulgaris*: catalytic electron transfer to rubrerythrin and two-iron superoxide reductase. *Arch Biochem Biophys* **394**:76-86.
8. Cypionka, H. 2000. Oxygen respiration by *Desulfovibrio* species. *Annu Rev Microbiol* **54**:827-48.
9. Cypionka, H., F. Widdel, and N. Pfennig. 1985. Survival of sulfate-reducing bacteria after oxygen stress, and growth in sulfate-free oxygen-sulfide gradients. *FEMS Microbiol Lett* **31**:39-45.
10. Das, A., E. D. Coulter, D. M. Kurtz, Jr., and L. G. Ljungdahl. 2001. Five-gene cluster in *Clostridium thermoaceticum* consisting of two divergent operons encoding rubredoxin oxidoreductase- rubredoxin and rubrerythrin-type A flavoprotein-high-molecular-weight rubredoxin. *J Bacteriol* **183**:1560-7.
11. Das, A., R. Silaghi-Dumitrescu, L. G. Ljungdahl, and D. M. Kurtz, Jr. 2005. Cytochrome bd oxidase, oxidative stress, and dioxygen tolerance of the strictly anaerobic bacterium *Moorella thermoacetica*. *J. Bacteriol.* **187**:2020-2029.
12. Dilling, W., and H. Cypionka. 1990. Aerobic respiration in sulfate-reducing bacteria. *FEMS Microbiol Lett* **71**:123-127.
13. Dolla, A., M. Fournier, and Z. Dermoun. 2006. Oxygen defense in sulfate-reducing bacteria. *J Biotechnol* **126**:87-100.
14. Emerson, J. P., E. D. Coulter, R. S. Phillips, and D. M. Kurtz, Jr. 2003. Kinetics of the superoxide reductase catalytic cycle. *J Biol Chem* **278**:39662-8.
15. Farr, S. B., and T. Kogoma. 1991. Oxidative stress responses in *Escherichia coli* and *Salmonella typhimurium*. *Microbiol Mol Biol Rev* **55**:561-585.
16. Fournier, M., C. Aubert, Z. Dermoun, M. C. Durand, D. Moinier, and A. Dolla. 2006. Response of the anaerobe *Desulfovibrio vulgaris* Hildenborough to oxidative conditions: proteome and transcript analysis. *Biochimie* **88**:85-94.

- 1 17. **Fournier, M., Z. Dermoun, M. C. Durand, and A. Dolla.** 2004. A new function of the
2 *Desulfovibrio vulgaris* Hildenborough [Fe] hydrogenase in the protection against
3 oxidative stress. *J Biol Chem* **279**:1787-93.
- 4 18. **Fournier, M., Y. Zhang, J. D. Wildschut, A. Dolla, J. K. Voordouw, D. C.**
5 **Schriemer, and G. Voordouw.** 2003. Function of oxygen resistance proteins in the
6 anaerobic, sulfate-reducing bacterium *Desulfovibrio vulgaris* Hildenborough. *J Bacteriol*
7 **185**:71-9.
- 8 19. **Gaballa, A., and J. D. Helmann.** 2002. A peroxide-induced zinc uptake system plays an
9 important role in protection against oxidative stress in *Bacillus subtilis*. *Mol Microbiol*
10 **45**:997-1005.
- 11 20. **Hardy, J., Hamilton, W. A.** 1981. The oxygen tolerance of sulfate-reducing bacteria
12 isolated from North Sea waters. *Current Microbiology* **6**:259-262.
- 13 21. **Hayashi, K., T. Ohsawa, K. Kobayashi, N. Ogasawara, and M. Ogura.** 2005. The
14 H₂O₂ stress-responsive regulator PerR positively regulates *srfA* expression in *Bacillus*
15 *subtilis*. *J Bacteriol* **187**:6659-67.
- 16 22. **He, Q., K. H. Huang, Z. He, E. J. Alm, M. W. Fields, T. C. Hazen, A. P. Arkin, J. D.**
17 **Wall, and J. Zhou.** 2006. Energetic consequences of nitrite stress in *Desulfovibrio*
18 *vulgaris* Hildenborough, inferred from global transcriptional analysis. *Appl Environ*
19 *Microbiol* **72**:4370-81.
- 20 23. **Heidelberg, J. F., R. Seshadri, S. A. Haveman, C. L. Hemme, I. T. Paulsen, J. F.**
21 **Kolonay, J. A. Eisen, N. Ward, B. Methe, L. M. Brinkac, S. C. Daugherty, R. T.**
22 **Deboy, R. J. Dodson, A. S. Durkin, R. Madupu, W. C. Nelson, S. A. Sullivan, D.**
23 **Fouts, D. H. Haft, J. Selengut, J. D. Peterson, T. M. Davidsen, N. Zafar, L. Zhou, D.**
24 **Radune, G. Dimitrov, M. Hance, K. Tran, H. Khouri, J. Gill, T. R. Utterback, T. V.**
25 **Feldblyum, J. D. Wall, G. Voordouw, and C. M. Fraser.** 2004. The genome sequence
26 of the anaerobic, sulfate-reducing bacterium *Desulfovibrio vulgaris* Hildenborough. *Nat*
27 *Biotechnol* **22**:554-9.
- 28 24. **Helmann, J. D., M. F. Wu, A. Gaballa, P. A. Kobel, M. M. Morshedi, P. Fawcett,**
29 **and C. Paddon.** 2003. The global transcriptional response of *Bacillus subtilis* to peroxide
30 stress is coordinated by three transcription factors. *J Bacteriol* **185**:243-53.
- 31 25. **Horsburgh, M. J., M. O. Clements, H. Crossley, E. Ingham, and S. J. Foster.** 2001.
32 PerR controls oxidative stress resistance and iron storage proteins and is required for
33 virulence in *Staphylococcus aureus*. *Infect Immun* **69**:3744-54.
- 34 26. **Imlay, J. A.** 2002. What biological purpose is served by superoxide reductase? *J Biol*
35 *Inorg Chem.* 2002 **7**:659-63.
- 36 27. **Jayaraman, A., P. J. Hallock, R. M. Carson, C. C. Lee, F. B. Mansfeld, and T. K.**
37 **Wood.** 1999. Inhibiting sulfate-reducing bacteria in biofilms on steel with antimicrobial
38 peptides generated in situ. *Appl Microbiol Biotechnol* **52**:267-75.
- 39 28. **Jenney, F. E., Jr., M. F. n. J. n. M. Verhagen, X. Cui, and M. W. n. W. Adams.** 1999.
40 Anaerobic microbes: oxygen detoxification without superoxide dismutase. *Science*
41 **286**:306-309.
- 42 29. **Joachimiak, M. P., J. L. Weisman, and B. May.** 2006. JColorGrid: software for the
43 visualization of biological measurements. *BMC Bioinformatics* **7**:225.
- 44 30. **Johnson, M. S., I. B. Zhulin, M. E. Gapuzan, and B. L. Taylor.** 1997. Oxygen-
45 dependent growth of the obligate anaerobe *Desulfovibrio vulgaris* Hildenborough. *J*
46 *Bacteriol* **179**:5598-601.

- 1 31. **Kepner, R. L., Jr., and J. R. Pratt.** 1994. Use of fluorochromes for direct enumeration
2 of total bacteria in environmental samples: past and present. *Microbiol Rev* **58**:603-15.
- 3 32. **Lehmann, Y., L. Meile, and M. Teuber.** 1996. Rubrerythrin from *Clostridium*
4 *perfringens*: cloning of the gene, purification of the protein, and characterization of its
5 superoxide dismutase function. *J Bacteriol* **178**:7152-8.
- 6 33. **Li, X., Z. He, and J. Zhou.** 2005. Selection of optimal oligonucleotide probes for
7 microarrays using multiple criteria, global alignment and parameter estimation. *Nucleic*
8 *Acids Res* **33**:6114-23.
- 9 34. **Lindqvist, A., J. Membrillo-Hernandez, R. K. Poole, and G. M. Cook.** 2000. Roles of
10 respiratory oxidases in protecting *Escherichia coli* K12 from oxidative stress. *Antonie*
11 *Van Leeuwenhoek* **78**:23-31.
- 12 35. **Lobo, Melo, Carita, Teixeira, and Saraiva.** 2007. The anaerobe *Desulfovibrio*
13 *desulfuricans* ATCC 27774 grows at nearly atmospheric oxygen levels. *FEBS Lett*
14 **581**:433-436.
- 15 36. **Lumppio, H. L., N. V. Shenvi, R. P. Garg, A. O. Summers, and D. M. Kurtz, Jr.**
16 1997. A rubrerythrin operon and nigerythrin gene in *Desulfovibrio vulgaris*
17 (Hildenborough). *J Bacteriol* **179**:4607-15.
- 18 37. **Lumppio, H. L., N. V. Shenvi, A. O. Summers, G. Voordouw, and D. M. Kurtz, Jr.**
19 2001. Rubrerythrin and rubredoxin oxidoreductase in *Desulfovibrio vulgaris*: a novel
20 oxidative stress protection system. *J Bacteriol* **183**:101-8.
- 21 38. **Machado, P., R. Felix, R. Rodrigues, S. Oliveira, and C. Rodrigues-Pousada.** 2006.
22 Characterization and expression analysis of the cytochrome bd oxidase operon from
23 *Desulfovibrio gigas*. *Curr Microbiol* **V52**:274-281.
- 24 39. **Mukhopadhyay, A., Z. He, E. J. Alm, A. P. Arkin, E. E. Baidoo, S. C. Borglin, W.**
25 **Chen, T. C. Hazen, Q. He, H.-Y. Holman, K. Huang, R. Huang, D. C. Joyner, N.**
26 **Katz, M. Keller, P. Oeller, A. Redding, J. Sun, J. Wall, J. Wei, Z. Yang, H.-C. Yen,**
27 **J. Zhou, and J. D. Keasling.** 2006. Salt stress in *Desulfovibrio vulgaris* Hildenborough:
28 an integrated genomics approach. *J. Bacteriol.* **188**:4068-4078.
- 29 40. **Nemati, M., G. E. Jenneman, and G. Voordouw.** 2001. Mechanistic study of microbial
30 control of hydrogen sulfide production in oil reservoirs. *Biotechnol Bioeng* **74**:424-34.
- 31 41. **Neria-Gonzalez, I., E. T. Wang, F. Ramirez, J. M. Romero, and C. Hernandez-**
32 **Rodriguez.** 2006. Characterization of bacterial community associated to biofilms of
33 corroded oil pipelines from the southeast of Mexico. *Anaerobe* **12**:122-33.
- 34 42. **Niviere, V., and M. Fontecave.** 2004. Discovery of superoxide reductase: an historical
35 perspective. *J Biol Inorg Chem* **9**:119-23.
- 36 43. **Noll, M., K. Petrukhin, and S. Lutsenko.** 1998. Identification of a novel transcription
37 regulator from *Proteus mirabilis*, PMTR, revealed a possible role of YJAI protein in
38 balancing zinc in *Escherichia coli*. *J Biol Chem* **273**:21393-21401.
- 39 44. **Podkopaeva, D. A., M. Grabovich, and G. A. Dubinina.** 2003. Oxidative stress and
40 antioxidant cell protection systems in the microaerophilic bacterium *Spirillum*
41 *winogradskii*. *Mikrobiologiya* **72**:600-8.
- 42 45. **Poole, R. K.** 1994. Oxygen reactions with bacterial oxidases and globins: binding,
43 reduction and regulation. *Antonie Van Leeuwenhoek* **65**:289-310.
- 44 46. **Postgate, J. R.** 1984. *The Sulfate-Reducing Bacteria*. Cambridge University Press,
45 Cambridge.

- 1 47. **Redding, A. M., A. Mukhopadhyay, D. C. Joyner, T. C. Hazen, and J. D. Keasling.**
2 2006. Study of nitrate stress in *Desulfovibrio vulgaris* Hildenborough using iTRAQ
3 proteomics. *Brief Funct Genomic Proteomic* **5**:133-143.
- 4 48. **Ricci, S., R. Janulczyk, and L. Bjorck.** 2002. The regulator PerR is involved in
5 oxidative stress response and iron homeostasis and is necessary for full virulence of
6 *Streptococcus pyogenes*. *Infect Immun* **70**:4968-76.
- 7 49. **Rodionov, D. A., I. Dubchak, A. Arkin, E. Alm, and M. S. Gelfand.** 2004.
8 Reconstruction of regulatory and metabolic pathways in metal-reducing delta-
9 proteobacteria. *Genome Biol* **5**:R90.
- 10 50. **Scott, C., H. Rawsthorne, M. Upadhyay, C. A. Shearman, M. J. Gasson, J. R. Guest,**
11 **and J. Green.** 2000. Zinc uptake, oxidative stress and the FNR-like proteins of
12 *Lactococcus lactis*. *FEMS Microbiol Lett* **192**:85-9.
- 13 51. **Tanaka, Y., M. Sogabe, K. Okumura, and R. Kurane.** 2002. A highly selective direct
14 method of detecting sulphate-reducing bacteria in crude oil. *Lett Appl Microbiol* **35**:242-
15 6.
- 16 52. **Tatusov, R. L., E. V. Koonin, and D. J. Lipman.** 1997. A genomic perspective on
17 protein families. *Science* **278**:631-7.
- 18 53. **Valentine JS, W. D., Lyons TJ, Liou LL, Goto JJ, Gralla EB.** 1998. The dark side of
19 dioxygen biochemistry. *Curr Opin Chem Biol.* **2**:253-62.
- 20 54. **Vincent, K. A., A. Parkin, O. Lenz, S. P. J. Albracht, J. C. Fontecilla-Camps, R.**
21 **Cammack, B. Friedrich, and F. A. Armstrong.** 2005. Electrochemical definitions of O₂
22 sensitivity and oxidative inactivation in hydrogenases. *J. Am. Chem. Soc.* **127**:18179-
23 18189.
- 24 55. **Voordouw, J. K., and G. Voordouw.** 1998. Deletion of the rbo gene increases the
25 oxygen sensitivity of the sulfate-reducing bacterium *Desulfovibrio vulgaris*
26 Hildenborough. *Appl Environ Microbiol* **64**:2882-7.
- 27 56. **Wang, G., P. Alamuri, and R. J. Maier.** 2006. The diverse antioxidant systems of
28 *Helicobacter pylori*. *Mol Microbiol* **61**:847-860.
- 29 57. **Wildschut, J. D., R. M. Lang, J. K. Voordouw, and G. Voordouw.** 2006.
30 Rubredoxin:oxygen oxidoreductase enhances survival of *Desulfovibrio vulgaris*
31 Hildenborough under microaerophilic conditions. *J. Bacteriol.* **188**:6253-6260.
- 32 58. **Wu, H. J., K. L. Seib, Y. N. Srikhanta, S. P. Kidd, J. L. Edwards, T. L. Maguire, S.**
33 **M. Grimmond, M. A. Apicella, A. G. McEwan, and M. P. Jennings.** 2006. PerR
34 controls Mn-dependent resistance to oxidative stress in *Neisseria gonorrhoeae*. *Mol*
35 *Microbiol* **60**:401-16.
- 36 59. **Zhang, W., D. E. Culley, M. Hogan, L. Vitiritti, and F. J. Brockman.** 2006. Oxidative
37 stress and heat-shock responses in *Desulfovibrio vulgaris* by genome-wide transcriptomic
38 analysis. *Antonie Van Leeuwenhoek* **90**:41-55.

Figure Captions

Figure 1. Overview of selected O₂ responsive proteins in *D. vulgaris*. (A) Localization and mechanistic role of individual proteins in O₂ reduction in the Gram negative *D. vulgaris* cell are shown. While all candidates are represented in the transcriptome data, those for which proteomics data was available are colored grey. Also shown is the Fenton's reaction between Fe²⁺ and H₂O₂ which generates harmful hydroxyl radicals. (B) The predicted PerR regulon (candidates with potential PerR binding motifs) and other selected candidates. Underlined genes are reported to encode NADH peroxidases. DVU numbers are shown in parentheses.

Figure 2. Effect of O₂ exposure on growth of *D. vulgaris*. Growth of *D. vulgaris* was measured via cell count / ml (AODC). Each measurement is an average of three technical replicates. (A) *D. vulgaris* cell counts after sparging (200 ml/min) with 0.05% O₂ in N₂ (open triangle), 0.1 % O₂ in N₂ (filled square), or N₂ (open square) measured over 60 hours. Over the 72 hour period, *D. vulgaris* showed similar growth profiles in 0.5% O₂ and N₂ (control), while in 0.1% O₂ a much lower maximal growth was observed. (B) *D. vulgaris* cell count after sparging (200 ml/min) with N₂ (open bar) compared to 0.1% O₂ (filled bar) at 0 and 240 minutes. In order to assess the cell wide changes initiated in response to the 0.1% O₂ exposure, biomass for transcript and protein analysis was collected at 240 min after initiation of exposure, prior to entering stationary phase. Note that the effect of 0.1% O₂ sparge is only evident at later time points.

Figure 3. Genes whose expression changed most significantly in response to 0.1% O₂ exposure (cut-off threshold of log₂ R ≥ 2 and corresponding Z ≥ 2). Heat map shows changes in mRNA

levels over time (in minutes) in response to either 0.1% O₂ or air stress. The range of changes observed for these two experiments are shown in the key as log₂ R adjacent to the heat map. * Predicted PerR regulon genes.

Figure 4. Transcriptomic response of selected genes in 0.1% O₂ and air exposed cultures. The heat map shows changes in mRNA levels over time (in minutes) in response to either 0.1% O₂ or air stress. Candidates are grouped by function or gene ID numbers and are not from an automated clustering. The range of changes observed for these two experiments are shown in the key adjacent to the heat map. Included candidates are genes considered important in redox changes, and genes for central pathways such as electron transport, ATP synthesis, carbon uptake and metabolism.

Figure 5. Transcriptomic response of signature SRB genes during 0.1% O₂ and air exposure. The heat map shows changes in mRNA levels over time in response to either 0.1% O₂ or air stress. Signature genes as described in Chhabra et al 2006 were used. Genes have been categorized by function. The range of changes observed for these two experiments are shown in the key adjacent to the heat map.

Figure 6. iTRAQ proteomics for exposure to 0.1% O₂ and air. **(A)** The 0.1% O₂-exposed sample was labeled with both tag₁₁₆ (replicate 1) and tag₁₁₇ (replicate 2), allowing the assessment of the internal error. **(B)** The plots shows log₂ (0.1% O₂/T0) vs. log₂ (N₂/T0). Proteins whose z-score $\geq |2|$ were considered significant, and these candidates are highlighted as shown in the legend. **(C)** Log₂(air/N₂) at 120 minutes compared to the log₂(air/N₂) at 240 minutes. Proteins

that have the same level of change in both time points would fall on the 45° line. Clustering of data around the 45° line demonstrated that there is a trend in changes observed between 120 minutes and 240 minutes. Selected proteins are color-coded as described in the legend.

Figure 7. Protein distribution in clusters of orthologous groups (COGs). Proteins identified in the proteomics data cover all major COG categories (except B and V, having 1 and 32 proteins, respectively). In each COG category, fraction of protein that showed an increase and decrease in the air stress is shown in hashed bars and filled bars respectively. The grey bar bars indicate the fraction of proteins identified and the bars with horizontal lines indicates fraction of the total predicted proteome belonging to that category. The COG categories are sorted in order of decreasing fraction identified (grey bar). Notably, the highest fraction of changes was observed in COG category S (function unknown). COGs R, L, U, and T appear under-represented. Category U contains many membrane proteins, which are often not present in high abundance. The low abundance of signaling proteins may also be the reason for disproportionately low identification of proteins in COG T. The label X represents all proteins with no assigned COG and is the largest fraction of the total proteome, containing 1066 proteins.

Figure 8. Comparison between proteomics and microarray data for selected candidates. This is a graphical representation of data presented in Table 1. Open symbols represent 0.1% O₂ exposure, whereas the solid symbols represent air exposure. Circle 1 highlights all of the candidates belonging to the low oxygen exposure. The most significant changes occurred in oxidative stress genes and in ZraP. Air exposure caused a much larger level of change. Circle 2 highlights the large increases observed in proteases and chaperones during air exposure. Circle 3

highlights the group of periplasmic binding ABC transport proteins that show an opposite trend, namely increased protein levels but decreased transcript levels. More candidates show this trend, compared to the few candidates that show increased transcript levels but decreased protein levels (top left hand quadrant).

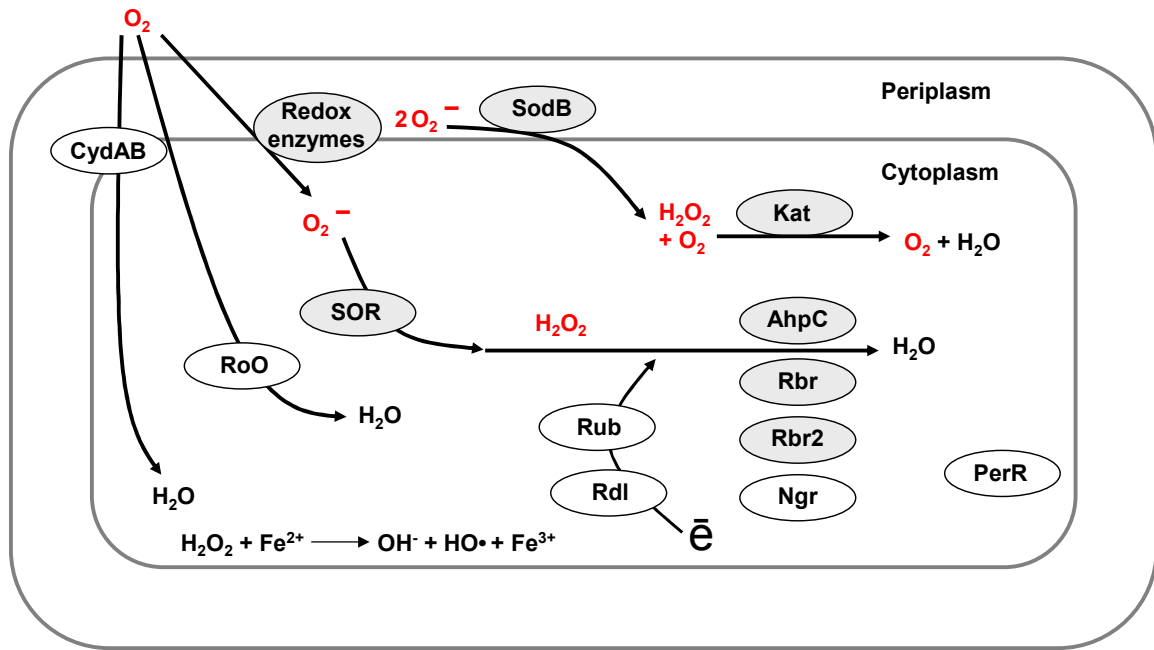
Figure 9. Analysis of microarray data to extract genes that show changes correlated with changes in the predicted PerR regulon. **(A)** Heat map shows changes in mRNA levels for the predicted members of the PerR regulon in 0.1% O₂ and air exposure. Average trend for each time point over all the members is shown in the bottom panel. The average values from **(A)** were used to search the entire data set. A Pearson correlation similarity measure showed 58 genes with a trend better than or equal to the worst fitting member of the PerR regulon (Supplementary Figure S4). **(B)** Heat map for mRNA changes for these 58 genes. Color legend indicates the predicted functional category of these genes. For complete details of this list, see Supplementary Table T1.

Figure 10. Microarray data for air stress. **(A)** Comparison of mRNA data for exposure to 0.1% O₂ vs. exposure air shows no linear relationship, (Pearson correlation coefficient = 0.03, p-value = 0.01805). **(B)** Comparison mRNA data of two biological replicates of air exposure at 240 min. Though exposure to air created a heterogeneous population, the responses from two different biological replicates correlate strongly (Pearson correlation coefficient value of 0.69, p-value < 0.000005). Note that data for the second biological replicate is from an independent experiment. **(C)** Heat shock (50°C, 120 min) data from (5) was compared with the 120 min air exposure data. Direct comparisons of these data were possible because both experiments used the same

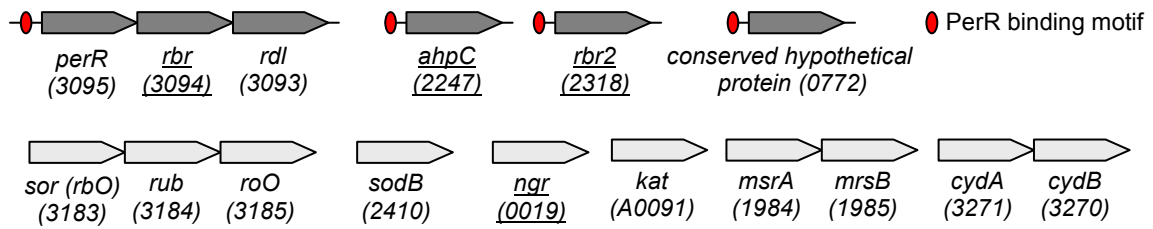
1 microarray design, the biomass samples came from the same pipeline, and the microarray
2 experiments used genomic DNA as control. A stronger linear relationship exists between the
3 overall trends observed for heat shock vs. air exposure (Pearson correlation coefficient value of
4 0.45, p-value < 0.000005). All p values are one-tailed t-statistic based.

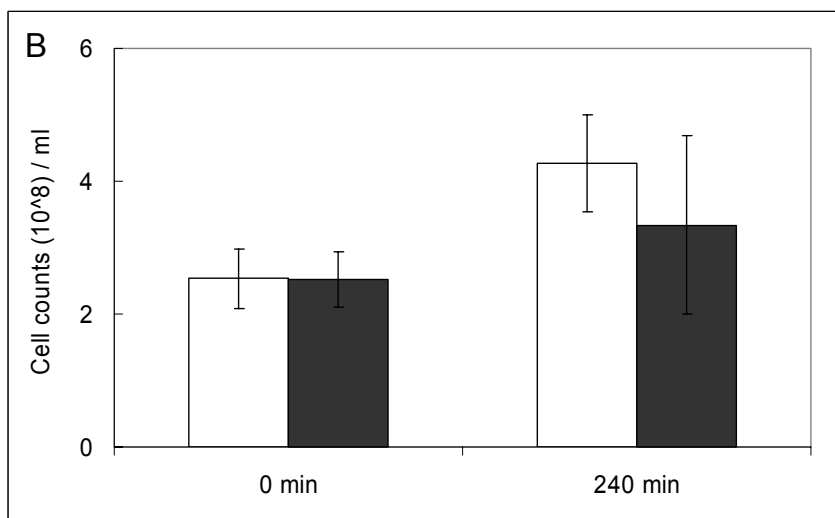
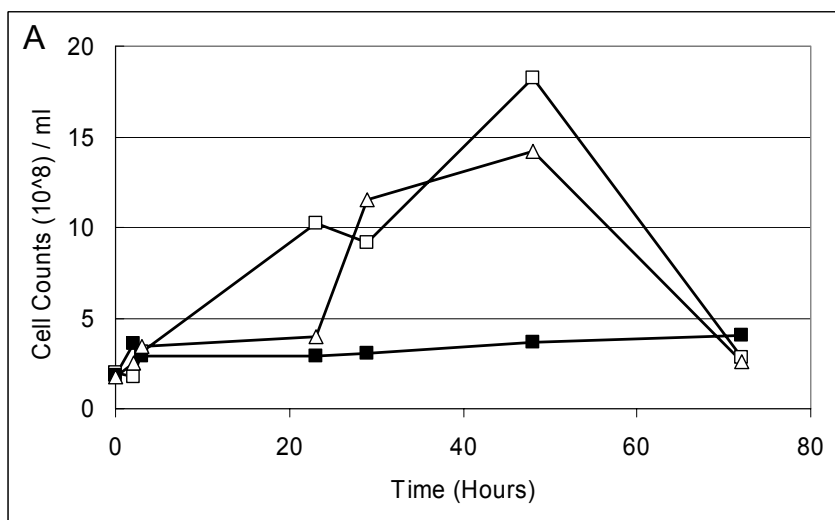
5

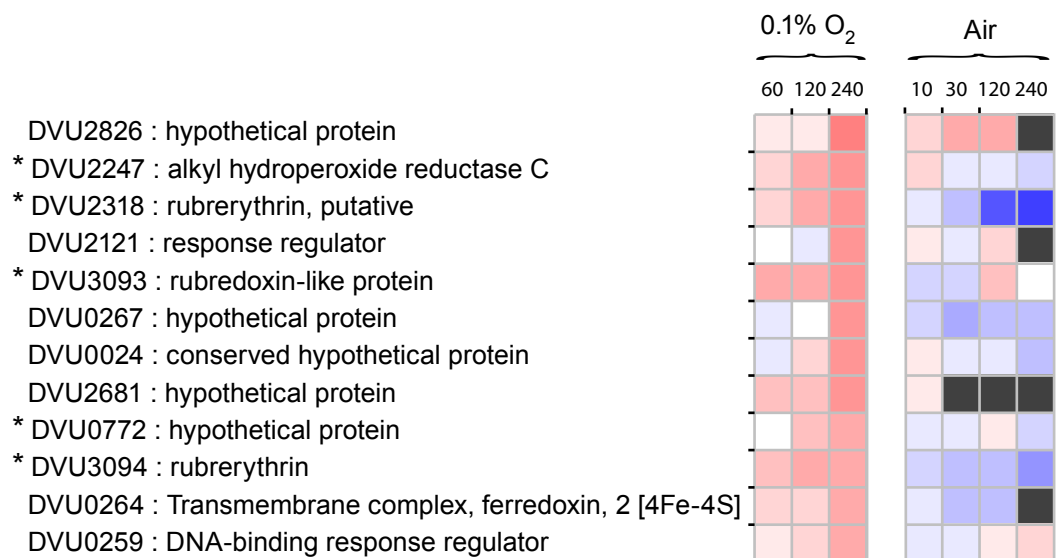
A



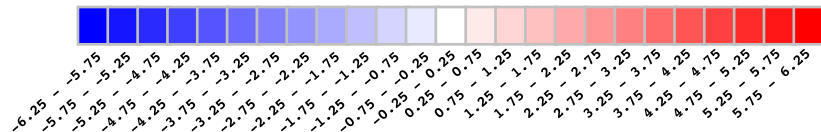
B







No data



DVU2410 : superoxide dismutase, Fe
 DVUA0091 : catalase
 DVU0019 : nigerythrin
 DVU1984 : peptide methionine sulfoxide reductase MsrA
 DVU1985 : conserved domain protein
 DVU1228 : thiol peroxidase
 DVU1839 : thioredoxin
 DVU1838 : thioredoxin reductase
 DVU1457 : thioredoxin reductase, putative
 DVU0378 : thioredoxin, putative

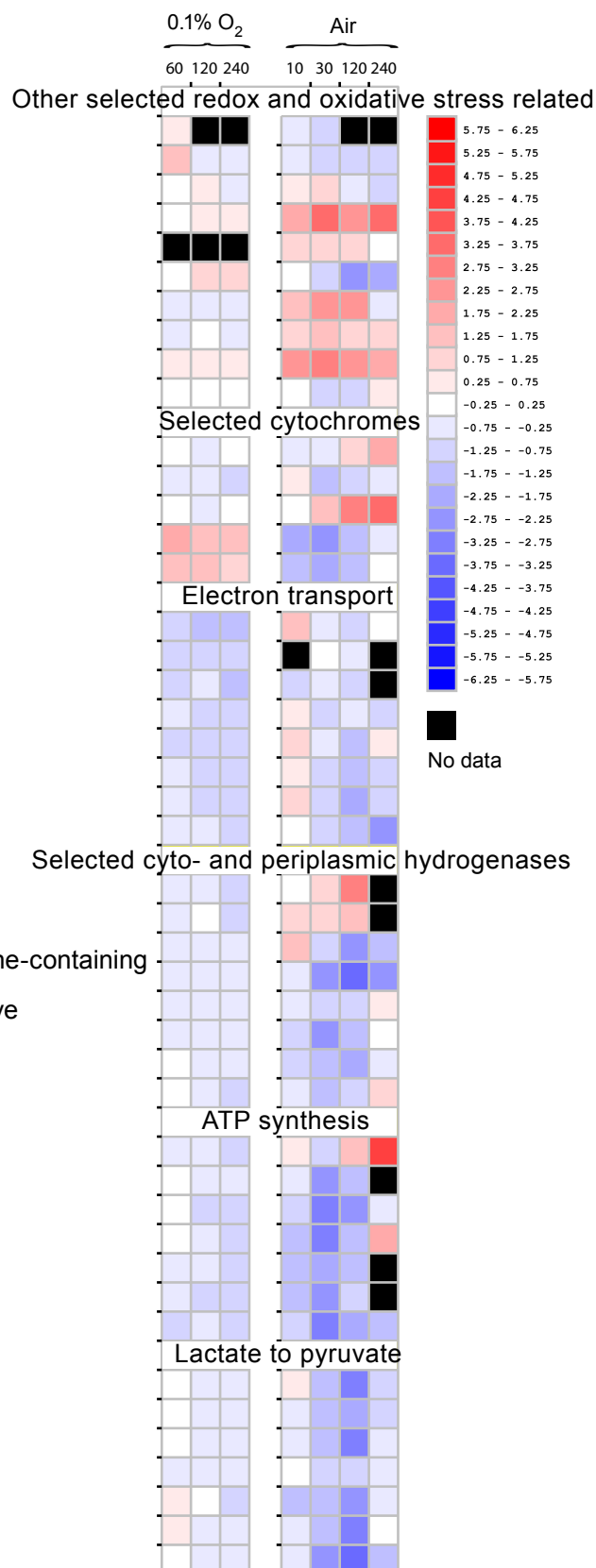
DVU2483 : cytochrome c family protein
 DVU0625 : cytochrome c nitrite reductase, catalytic subunit NrfA, putative
 DVU2809 : cytochrome c3
 DVU3271 : cytochrome d ubiquinol oxidase, subunit I
 DVU3270 : cytochrome d ubiquinol oxidase, subunit II

DVU0536 : HmcA; high-molecular-weight cytochrome c
 DVU0535 : 40.1 kd protein in hmc operon (HmcB)
 DVU0534 : HmcC, 43.2 kd protein in hmc operon
 DVU0533 : HmcD, 5.8 kd protein in hmc operon
 DVU0532 : HmcE, 25.3 kd protein in hmc operon
 DVU0531 : HmcF, 52.7 kd protein in hmc operon
 DVU0530 : Rrf1 protein
 DVU0529 : Rrf2 protein

DVU1770 : periplasmic [Fe] hydrogenase, small subunit
 DVU2526 : periplasmic [NiFe] hydrogenase, large subunit, isozyme 2
 DVU1918 : periplasmic [NiFeSe] hydrogenase, large subunit, selenocysteine-containing
 DVU1917 : periplasmic [NiFeSe] hydrogenase, small subunit
 DVU2287 : hydrogenase, CooK subunit, selenocysteine-containing, putative
 DVU2286 : hydrogenase, CooM subunit, putative
 DVU2290 : hydrogenase, CooU subunit, putative
 DVU2289 : hydrogenase, CooX subunit, putative

DVU0774 : ATP synthase, F1 epsilon subunit
 DVU0775 : ATP synthase, F1 beta subunit
 DVU0776 : ATP synthase, F1 gamma subunit
 DVU0777 : ATP synthase, F1 alpha subunit
 DVU0778 : ATP synthase, F1 delta subunit
 DVU0779 : ATP synthase F0, B subunit, putative
 DVU0780 : ATP synthase F0, B subunit, putative

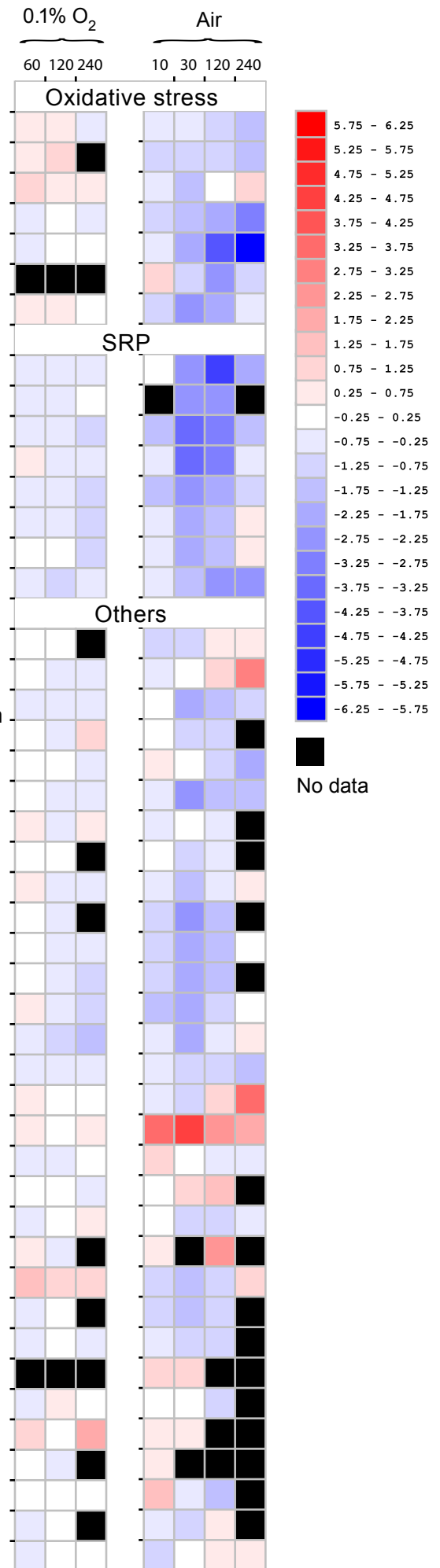
DVU3025 : pyruvate-ferredoxin oxidoreductase
 DVU3026 : L-lactate permease family protein
 DVU3027 : glycolate oxidase, subunit GlcD
 DVU3028 : iron-sulfur cluster-binding protein
 DVU3029 : phosphate acetyltransferase
 DVU3030 : acetate kinase
 DVU3024 : hypothetical protein

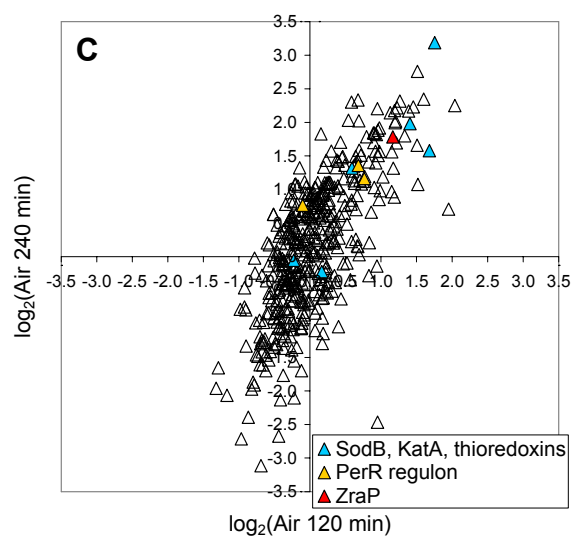
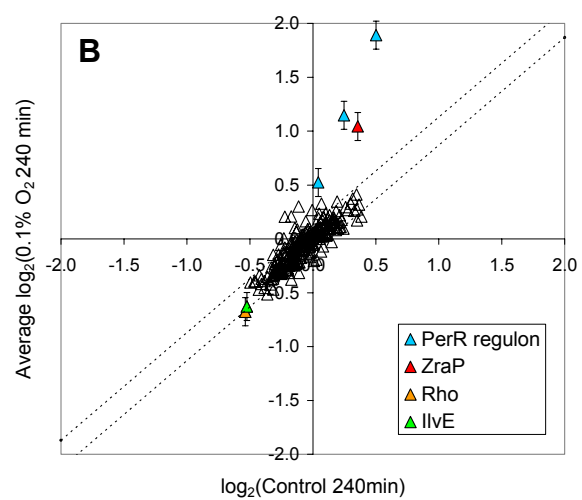
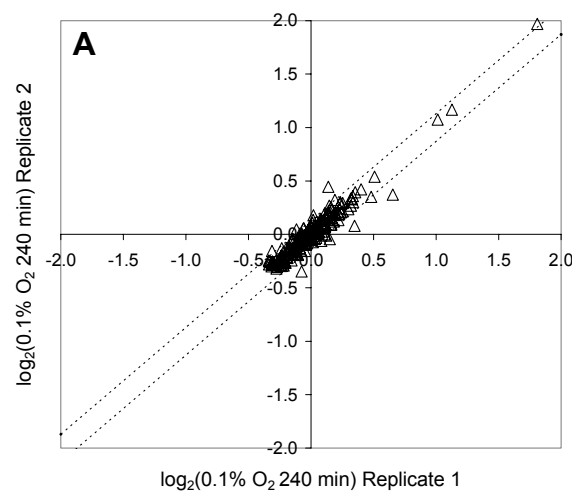


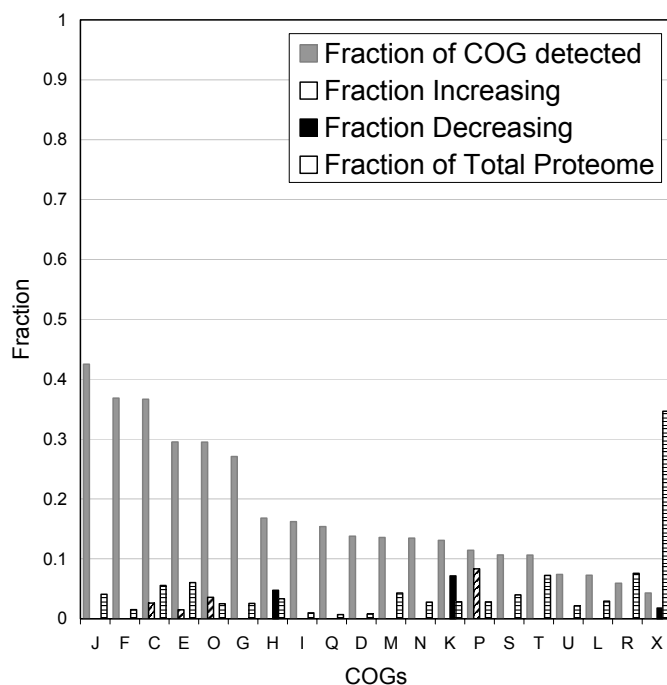
DVU3183 : desulfoferrodoxin
DVU3184 : rubredoxin
DVU3185 : rubredoxin-oxygen oxidoreductase
DVU0883 : glutaredoxin, putative
DVU0305 : ferredoxin II
DVU3276 : ferredoxin I
DVU1568 : ferritin

DVU0402 : dissimilatory sulfite reductase alpha subunit
DVU0403 : dissimilatory sulfite reductase beta subunit
DVU0846 : adenylylsulphate reductase, beta subunit
DVU0847 : adenylyl-sulphate reductase, alpha subunit
DVU0848 : Quinone-interacting membrane-bound oxidoreductase
DVU0849 : Quinone-interacting membrane-bound oxidoreductase
DVU0850 : Quinone-interacting membrane-bound oxidoreductase
DVU2776 : dissimilatory sulfite reductase, gamma subunit

DVU0105 : glutamine ABC transporter, ATP-binding protein
DVU0162 : carbamoyl-phosphate synthase, large subunit
DVU0386 : amino acid ABC transporter, periplasmic amino acid-binding protein
DVU0405 : cobyrinic acid a,c-diamide synthase
DVU0456 : DHH family protein
DVU1067 : membrane protein, Bmp family
DVU1069 : branched chain amino acid ABC transporter, permease protein
DVU1070 : branched chain amino acid ABC transporter, ATP-binding protein
DVU1286 : Integral membrane protein
DVU1287 : Periplasmic (Tat), binds 2[4Fe-4S]
DVU1288 : Periplasmic (Sec) triheme cytochrome c
DVU1289 : Cytoplasmic, binds 2 [4Fe-4S]
DVU1290 : Inner membrane protein binds 2 heme b
DVU1636 : inorganic pyrophosphatase, manganese-dependent
DVU1867 : diaminopimelate epimerase
DVU2108 : MTH1175-like domain family protein
DVU2310 : metallo-beta-lactamase family protein
DVU2735 : phenylacetate-coenzyme A ligase
DVU2825 : pyruvate formate-lyase 1 activating enzyme, putative
DVU3212 : pyridine nucleotide-disulfide oxidoreductase
DVU3290 : conserved domain protein
DVU3379 : ribonucleoside-diphosphate reductase
DVU0884 : conserved hypothetical protein
DVU0951 : molybdopterin biosynthesis MoeA protein, putative
ORF00713 : branched-chain amino acid ABC transporter, permease protein
DVU2103 : iron-sulfur cluster-binding/ATPase domain protein
DVU2271 : pyruvate formate-lyase activating enzyme, putative
ORF02867 : amino acid ABC transporter, ATP-binding protein
DVU2422 : nitroreductase family protein
DVU2990 : molybdopterin biosynthesis MoeA protein
DVU3113 : carbamoyl-phosphate synthase, small subunit

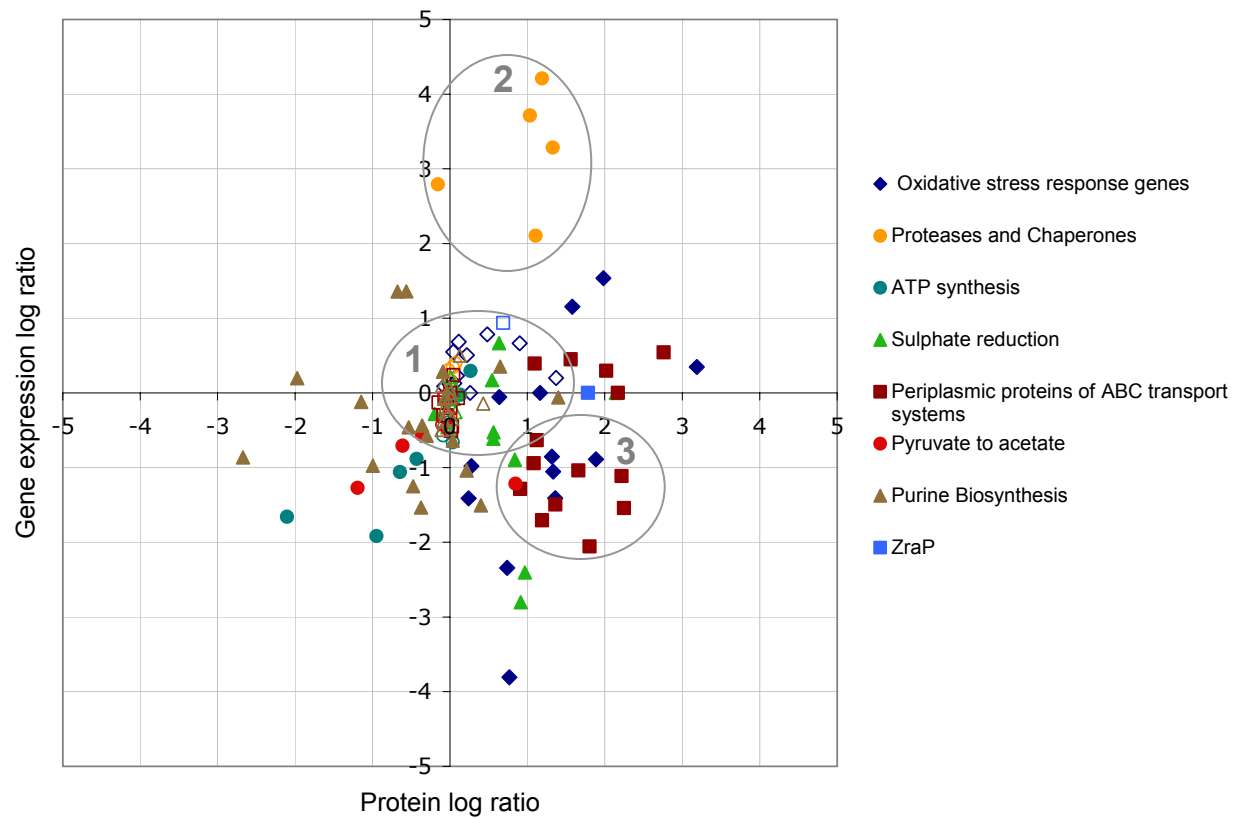


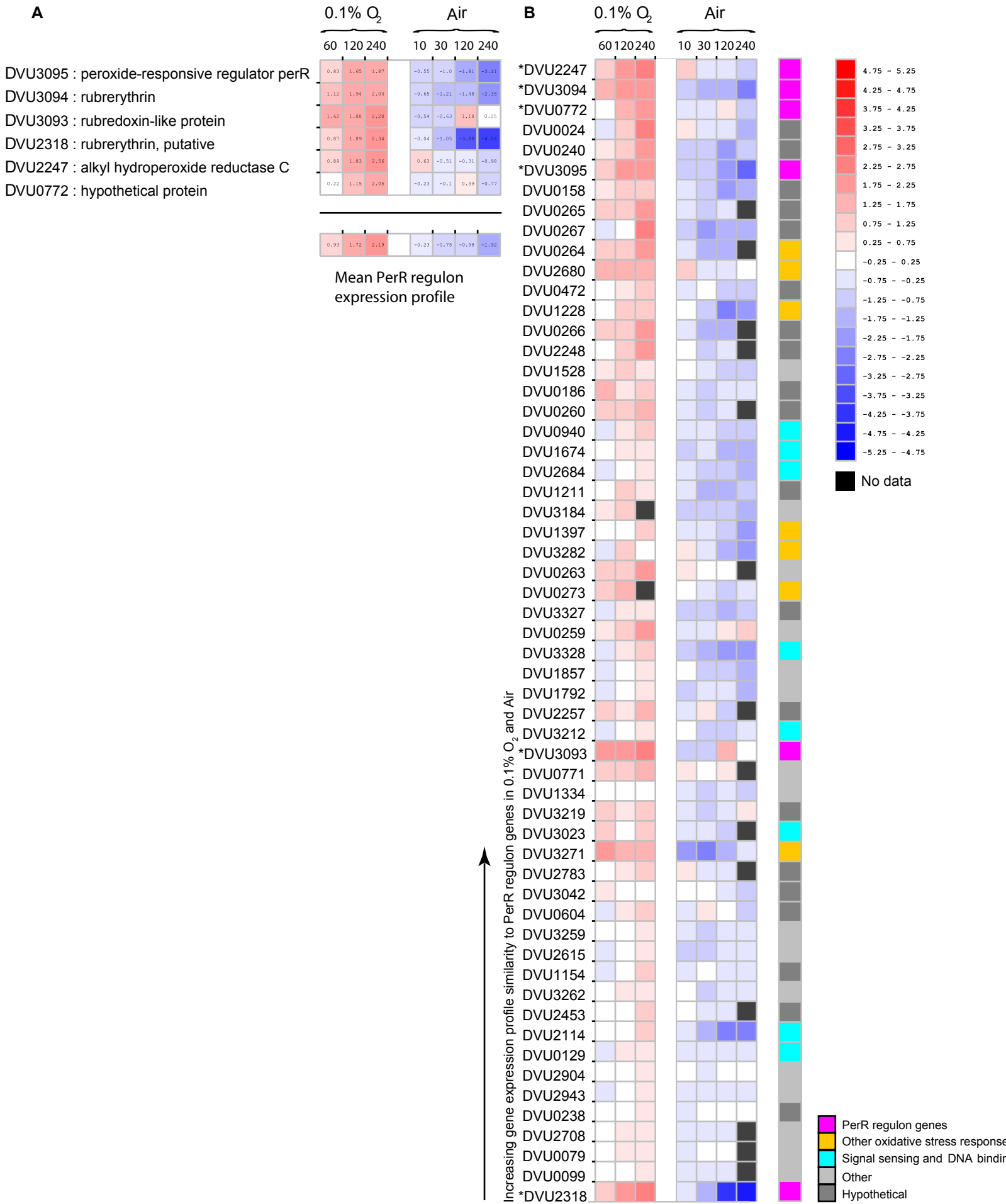




COG Category Description

- B: Chromatin structure and dynamics
- C: Energy production and conversion
- D: Cell division and chromosome partitioning
- E: Amino acid transport and metabolism
- F: Nucleotide transport and metabolism
- G: Carbohydrate transport and metabolism
- H: Coenzyme metabolism
- I: Lipid metabolism
- J: Translation, ribosomal structure and biogenesis
- K: Transcription
- L: DNA replication, recombination, and repair
- M: Cell envelope biogenesis, outer membrane
- N: Cell motility and secretion
- O: Posttranslational modification, protein turnover, chaperones
- P: Inorganic ion transport and metabolism
- Q: Secondary metabolites biosynthesis, transport, and catabolism
- R: General function prediction only
- S: Function unknown
- T: Signal transduction mechanisms
- U: Intracellular trafficking and secretion
- V: Defense mechanisms
- X: No annotated COG function





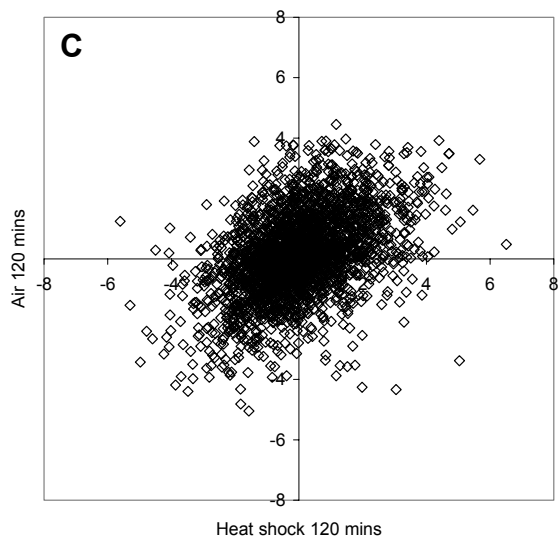
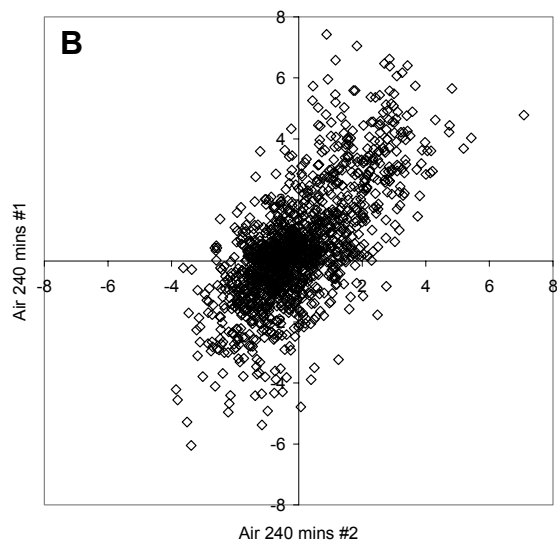
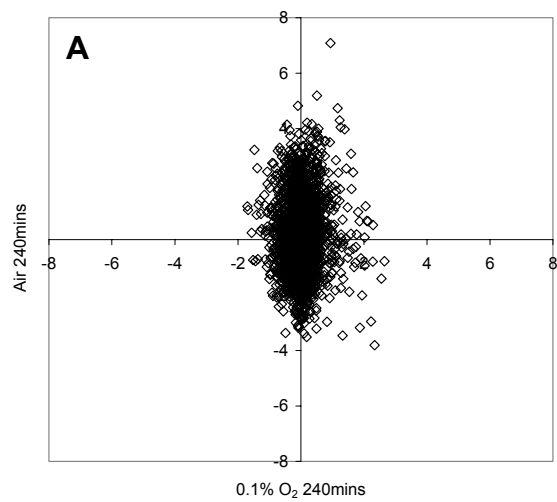


Table 1. Selected Proteomics data.

DVU#	Gene name	Description	iTRAQ Log ₂ (0.1% O ₂ / control) 240mins (± 0.13) ^{a, b}	Microarray Log ₂ (0.1% O ₂ / control) 240mins ^b	iTRAQ Log ₂ (Air / control) 240mins (± 0.13) ^{a, b}	Microarray Log ₂ (air / control) 240mins ^b
Oxidative stress response proteins						
DVU0995	-	ThiJ/Pfpl family protein	--	0.42 (0.8)	1.33 (1.16)	-1.05 (-1.89)
DVU1228	tpX	thiol peroxidase	0.16 (0.77)	0.5 (0.84)	0.24 (0.09)	-1.41 (-2.54)
DVU1397	bfr	bacterioferritin	-0.02 (0.05)	0.12 (0.22)	0.28 (0.13)	-0.98 (-1.18)
DVU1457	trxB	thioredoxin reductase, putative	0.15 (0.75)	0.11 (0.22)	1.98 (1.79)	1.53 (2.75)
DVU1568	ftn	ferritin	-0.13 (-0.38)	0.22 (0.38)	0.74 (0.58)	-2.34 (-4.3)
DVU1839	trx	thioredoxin	0.14 (0.7)	-0.1 (-0.18)	1.58 (1.4)	1.15 (1.84)
DVU2247	ahpC	alkyl hydroperoxide reductase C	1.89 (7.41)	0.19 (0.35)	1.36 (1.18)	-1.4 (0)
DVU2318	rbr2	rubrerythrin, putative	1.14 (4.56)	0.66 (1.13)	0.77 (0.6)	-3.8 (0)
DVU2410	sodB	superoxide dismutase, Fe	0.32 (1.4)	--	3.19 (2.97)	0.34 (0)
DVU3049	-	hemerythrin family protein	0.27 (1.19)	0.08 (0.14)	1.88 (1.7)	-0.89 (-1.41)
DVU3094	rbr	rubrerythrin	0.52 (2.16)	0.78 (1.36)	1.16 (0.99)	--
DVU3183	SOR	Superoxide reductase	--	0.59 (1.09)	1.69 (1.51)	2.31 (1.69)
DVU3185	roO	rubredoxin-oxygen oxidoreductase	0 (0.11)	0.54 (1.03)	0.64 (0.48)	-0.05 (-0.1)
DVUA0091	kat	Catalase	0.19 (0.9)	0.68 (0.84)	1.32 (1.14)	-0.85 (-1.25)
Proteases and Chaperons and other stress response						
DVU0811	dnaK	dnaK	0.03 (0.26)	0.24 (0.39)	1.03 (0.87)	3.28 (5.62)
DVU1012	-	hemolysin-type calcium-binding repeat	-0.39 (-1.37)	0.3 (0.45)	1.19 (1.02)	3.71 (0)
DVU1468	htrA	peptidase/PDZ domain	-0.36 (-1.27)	0.39 (0.74)	1.11 (0.94)	4.21 (6.74)
DVU1976	groEL	chaperonin, 60 kDa	-0.35 (-1.21)	0.34 (0.47)	-0.16 (-0.3)	2.1 (3.82)
DVU1977	groES	chaperonin, 10 kDa	--	0.15 (0.25)	1.33 (1.15)	2.79 (3.63)
DVU3384	zraP	zinc resistance-associated protein	1.04 (4.16)	0.93 (1.24)	1.78 (1.6)	--
Periplasmic proteins of ABC transport systems.						
DVU0095	potD-1	polyamine ABC transporter, periplasmic polyamine-binding	--	-0.5 (-0.84)	1.56 (1.38)	0.44 (0.81)
DVU0107	glnH	glutamine ABC transporter, periplasmic glutamine-binding	--	-0.1 (-0.19)	2.25 (2.05)	-1.54 (-2.74)
DVU0169	-	oligopeptide/dipeptide ABC transporter, periplasmic	0.09 (0.49)	-0.2 (-0.3)	2.22 (2.02)	-1.11 (-1.54)
DVU0386	glnH	amino acid ABC transporter, periplasmic	0.12 (0.62)	-0.44 (-0.77)	1.36 (1.18)	-1.49 (-2.82)
DVU0547	-	high-affinity branched chain amino acid ABC transporter, periplasmic	0.04 (0.3)	-0.29 (-0.51)	1.19 (1.02)	-1.7 (-3.33)
DVU0675	flhY	amino acid ABC transporter, periplasmic	0.22 (0.97)	--	2.17 (1.97)	--
DVU0712	-	amino acid ABC transporter, periplasmic-binding	0.25 (1.14)	-0.07 (-0.14)	1.08 (0.91)	-0.94 (0)
DVU0752	-	amino acid ABC transporter	-0.28 (-0.97)	-0.3 (-0.55)	1.1 (0.92)	0.39 (0.7)
DVU0966	-	amino acid ABC transporter, periplasmic	-0.14 (-0.41)	-0.5 (-0.92)	1.8 (1.62)	-2.05 (-3.6)
DVU1238	-	amino acid ABC transporter, periplasmic	--	-0.3 (-0.59)	1.66 (1.48)	-1.04 (-1.96)
DVU1937	-	phosphonate ABC transporter, periplasmic	-0.04 (-0.02)	-0.06 (-0.12)	0.91 (0.74)	-1.28 (-2.3)
DVU2297	-	glycine/betaine/L-proline ABC transporter, periplasmic-binding	0 (0.12)	0.23 (0.38)	2.02 (1.83)	0.29 (0.55)
DVU2342	-	amino acid ABC transporter, periplasmic	--	-0.51 (-0.93)	1.12 (0.95)	-0.63 (-1.03)
DVU3162	-	ABC transporter, periplasmic substrate-binding protein	0.09 (0.51)	-0.13 (-0.24)	2.76 (2.55)	0.54 (0)
ATP synthesis						
DVU0775	atpD	ATP synthase, F1 beta subunit	-0.21 (-0.68)	-0.39 (-0.63)	0.27 (0.11)	0.29 (0.35)
DVU0777	atpA	ATP synthase, F1 alpha subunit	-0.13 (-0.38)	-0.57 (-0.97)	0.13 (-0.01)	-0.02 (-0.02)
DVU0778	atpH	ATP synthase, F1 delta subunit	-0.24 (-0.78)	-0.66 (-0.94)	-0.43 (-0.57)	-0.88 (-1.42)
DVU0114	hisG	ATP phosphoribosyltransferase	--	-0.2 (-0.21)	-2.1 (-2.2)	-1.65 (-3.21)
DVU0779	atpF2	ATP synthase F0, B subunit	--	-0.89 (-1.56)	-0.64 (-0.78)	-1.06 (-1.17)
DVU0780	atpF1	ATP synthase F0, B subunit	--	-0.39 (-0.69)	-0.95 (-1.07)	-1.91 (-2.97)
Sulphate reduction						
DVU0402	dsrA	dissimilatory sulfite reductase alpha subunit	0.05 (0.35)	0.09 (0.17)	0.97 (0.8)	-2.4 (-2.49)
DVU0403	dvsB	dissimilatory sulfite reductase beta subunit	0.22 (1)	0.01 (0.01)	0.91 (0.75)	-2.8 (-4.74)
DVU0404	dsrD	dissimilatory sulfite reductase D	-0.02 (0.04)	0.2 (0.3)	2.14 (1.95)	--
DVU0847	apsA	adenylyl-sulphate reductase, alpha subunit	0.02 (0.25)	-0.08 (-0.13)	0.84 (0.67)	-0.89 (-1.32)
DVU0848	qmoA	Quinone-interacting membrane-bound oxidoreductase	-0.03 (0)	-0.5 (-0.89)	0.56 (0.4)	-0.61 (-1)
DVU0849	qmoB	Quinone-interacting membrane-bound oxidoreductase	-0.1 (-0.27)	-0.46 (-0.67)	0.54 (0.39)	0.16 (0.26)
DVU1295	sat	sulfate adenylyltransferase	0.07 (0.42)	-0.08 (-0.14)	-0.19 (-0.34)	-0.28 (0)
DVU1597	sir	sulfite reductase, assimilatory-type	-0.37 (-1.3)	-0.05 (-0.1)	0.63 (0.47)	0.66 (1.22)
DVU2776	dsrC	dissimilatory sulfite reductase, gamma subunit	-0.23 (-0.76)	-0.25 (-0.44)	0.56 (0.41)	-0.52 (-0.57)
Purine Biosynthesis						
DVU0161	purF	amidophosphoribosyltransferase	--	-0.22 (-0.37)	-0.36 (-0.5)	-0.43 (-0.72)
DVU0488	purD	phosphoribosylamine-glycine ligase	0.31 (1.37)	-0.06 (-0.08)	-0.56 (-0.7)	1.36 (0)
DVU0795	purC	phosphoribosylaminoimidazole-succinocarboxamide synthase	-0.02 (0.03)	-0.34 (-0.52)	-0.09 (-0.23)	0.28 (0.45)
DVU1043	guaA	GMP synthase	--	0.02 (0.03)	-0.68 (-0.81)	1.35 (2.62)
DVU1044	guaB	inosine-5'-monophosphate dehydrogenase	-0.21 (-0.7)	0.09 (0.15)	-1.15 (-1.26)	-0.12 (-0.21)
DVU1406	purM	phosphoribosylformylglycinamide cyclo-ligase	--	-0.33 (-0.63)	-0.48 (-0.61)	-1.25 (-1.65)
DVU1932	adk	adenylate kinase (TIGR)	0.11 (0.57)	-0.49 (-0.68)	0.4 (0.24)	-1.5 (-2.97)
DVU2942	purB	adenylosuccinate lyase	0.2 (0.93)	-0.14 (-0.24)	0.65 (0.49)	0.35 (0.53)
DVU3181	purL	phosphoribosylformylglycinamide synthase II	0.04 (0.32)	-0.18 (-0.28)	-1.97 (-2.07)	0.19 (0.34)
DVU3204	purA	adenylosuccinate synthetase	0 (0.11)	--	0.04 (-0.11)	-0.64 (-1.16)
DVU3206	purH	phosphoribosylaminoimidazolecarboxamide formyltransferase	--	0.28 (0.5)	-0.37 (-0.51)	-1.53 (-3.02)
DVU3235	purH	IMP cyclohydrolase, putative	0.26 (1.17)	0.06 (0.11)	1.4 (1.22)	-0.06 (-0.11)
Pyruvate to acetate						
DVU3025	por	pyruvate-ferredoxin oxidoreductase	-0.3 (-1.03)	-0.04 (-0.07)	-0.36 (-0.5)	-0.56 (-0.8)
DVU3027	gldD	glycolate oxidase, subunit	-0.23 (-0.75)	-0.42 (-0.77)	-0.61 (-0.74)	-0.7 (-0.81)
DVU3029	pta	phosphate acetyltransferase	-0.29 (-1)	-0.47 (-0.81)	-1.19 (-1.31)	-1.27 (0)
DVU3030	ackA	acetate kinase	0 (0.16)	-0.31 (-0.54)	0.85 (0.68)	-1.21 (-1.36)

^a ± 0.13 represents the internal error cut-off as computed in the methods section^b Values shown are log₂ ratios, in paranthesis are the corresponding z-scores; only values for which z-score is ≥ 2 were considered significant change